BRICK and Beyond: Bayesian analyses of low-energy ^{3}He-^{4}He data using R-matrix and Effective Field Theory

Daniel Phillips

Ohio University

with Daniel Odell, Carl Brune,
James deBoer, Som Paneru,
Mahesh Poudel, & Andrius Burnelis

Research supported by the DOE Office of Science, the SSAP, and the NSF OAC

Outline

- Bayes' theorem in one slide
- Bayesian R-matrix analysis of $^3He + ^4He \to ^7Be + \gamma$ and $^3He + ^4He$ elastic scattering
    - Set up: data + model

      Odell, Brune, DP, deBoer, Paneru,Frontiers in Physics (2022)
      Paneru, Brune Connolly, Odell, Poudel, DP, et al. Phys. Rev. C (2024)
    - Experimental imperfections
    - Why the full posterior?
    - Error propagation
- EFT modeling of $He + ^4He \to ^7Be + \gamma$ and $^3He + ^4He$ elastic scattering
    - What does the EFT amplitude for these reactions look like?
    - Low-energy S-factor data

      Zhang, Nollett, DP, J. Phys. G (2020)
      Poudel, DP, J. Phys. G. (2022)
      Burnelis, DP
    - What about scattering data?
- Summary and Future Work

The Bayes-ics

Thomas Bayes (1701?-1761)

http://www.bayesian-inference.com

$$\mathrm{pr}(A|B,I) = \frac{\mathrm{pr}(B|A,I)\mathrm{pr}(A|I)}{\mathrm{pr}(B|I)}$$

The Bayes-ics

Thomas Bayes (1701?-1761)

http://www.bayesian-inference.com

Probability as degree of belief

$$\mathrm{pr}(A|B,I) = \frac{\mathrm{pr}(B|A,I)\mathrm{pr}(A|I)}{\mathrm{pr}(B|I)}$$

$$\mathrm{pr}(\vec{\theta}\,|\,D,I) = \frac{\mathrm{pr}(D\,|\,\vec{\theta},I)\mathrm{pr}(\vec{\theta}\,|\,I)}{\mathrm{pr}(D\,|\,I)}$$

The Bayes-ics

Thomas Bayes (1701?-1761)

http://www.bayesian-inference.com

Probability as degree of belief

$$\mathrm{pr}(A|B,I) = \frac{\mathrm{pr}(B|A,I)\,\mathrm{pr}(A|I)}{\mathrm{pr}(B|I)}$$

Likelihood

Prior

$$\mathrm{pr}(\vec{\theta}\,|\,D,I) = \frac{\mathrm{pr}(D\,|\,\vec{\theta},I)\,\mathrm{pr}(\vec{\theta}\,|\,I)}{\mathrm{pr}(D\,|\,I)}$$

Posterior

Model evidence

The Bayes-ics

Thomas Bayes (1701?-1761)

http://www.bayesian-inference.com

Probability as degree of belief

$$\mathrm{pr}(A|B,I) = \frac{\mathrm{pr}(B|A,I)\mathrm{pr}(A|I)}{\mathrm{pr}(B|I)}$$

Likelihood

Prior

$$\mathrm{pr}(\vec{\theta}\,|\,D,I) = \frac{\mathrm{pr}(D\,|\,\vec{\theta},I)\mathrm{pr}(\vec{\theta}\,|\,I)}{\mathrm{pr}(D\,|\,I)}$$

Posterior

Model evidence

Typically evaluated by MCMC sampling

The Bayes-ics

Thomas Bayes (1701?-1761)

http://www.bayesian-inference.com

Probability as degree of belief

$$\mathrm{pr}(A|B,I) = \frac{\mathrm{pr}(B|A,I)\mathrm{pr}(A|I)}{\mathrm{pr}(B|I)}$$

Likelihood ↓ Prior ↓

$$\mathrm{pr}(\vec{\theta}\,|\,D,I) = \frac{\mathrm{pr}(D\,|\,\vec{\theta},I)\mathrm{pr}(\vec{\theta}\,|\,I)}{\mathrm{pr}(D\,|\,I)}$$

↑ Posterior ↑ Model evidence

Typically evaluated by MCMC sampling

Marginalization: $\mathrm{pr}(x|\mathrm{data},I) = \int dy\,\mathrm{pr}(x,y|\mathrm{data},I)$

Allows us to integrate out "nuisance" parameters, e.g., those associated with systematic uncertainties

SONIK data set

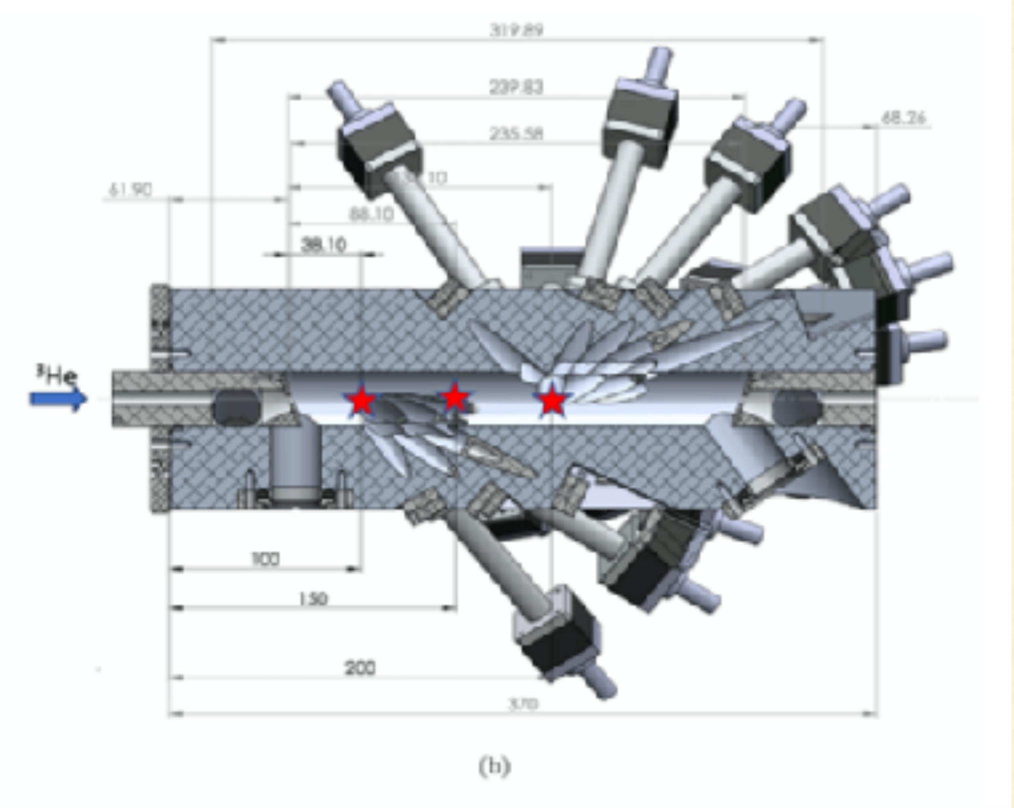

Paneru et al., Phys. Rev. C (2024)

- ^{3}He beam incident on SONIK apparatus
- Intensity of about 10^{12} s^{-1}
- Windowless gas target
- Measured at nine beam energies E[^{3}He]=0.721-5.490 MeV
- Three different interaction regions, corresponding to slightly different c.m. energies of the collision
- Total systematic uncertainties that are independent of energy and angle estimated at 2%
- Telescopes have a 1.6% variation of aperture around mean value, so acceptance correction is angle dependent
- Consistent with older, Barnard data set at higher energies

Full data set for model calibration

- 88 S-factor data
  - Seattle (S)
  - Weizmann
  - Luna (L)
  - Erna
  - Notre Dame
  - Atomki
- Plus 34 branching-ratio data

- Scattering data
  - SONIK: 451 from 0.385 to 3.127 MeV
  - Barnard: 646 from 1.49 to 3.27 MeV

Full data set for model calibration

- 88 S-factor data
  - Seattle (S)
  - Weizmann
  - Luna (L)
  - Erna
  - Notre Dame
  - Atomki
- Plus 34 branching-ratio data

- Scattering data
  - SONIK: 451 from 0.385 to 3.127 MeV
  - Barnard: 646 from 1.49 to 3.27 MeV

- Specify CMEs
  - SONIK: by energy
  - Barnard: 5%
  - S-factor: by set
  - Branching ratio: none

Full data set for model calibration

- 88 S-factor data
  - Seattle (S)
  - Weizmann
  - Luna (L)
  - Erna
  - Notre Dame
  - Atomki
- Plus 34 branching-ratio data

- Scattering data
  - SONIK: 451 from 0.385 to 3.127 MeV
  - Barnard: 646 from 1.49 to 3.27 MeV

- Specify CMEs
  - SONIK: by energy
  - Barnard: 5%
  - S-factor: by set
  - Branching ratio: none

Two analyses:

Capture + SONIK

Capture + SONIK + Barnard

R-matrix model

Odell, Brune, DP, deBoer, Paneru, Frontiers in Physics (2022)

- Goal: describe scattering and capture data up to the p^{6}Li threshold
- 3/2- and 1/2- bound states with prior ranges for ANCs from 1 to 5 MeV

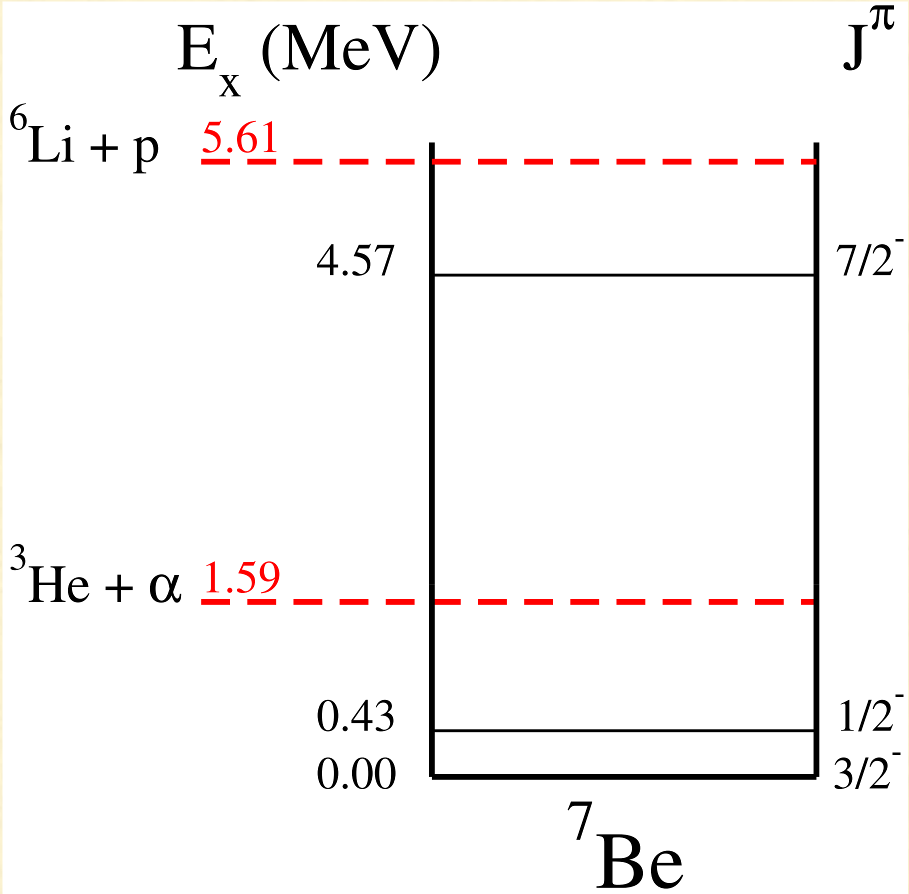

Background & resonance levels

	E (MeV)	Γ_α (MeV)
1/2-	21.6	[-200.200]
3/2-	21.6	[-100,100]
5/2-	7	[0,100]
7/2-	[2,10]	[0,10]
1/2+	14	[0,100]
3/2+	12	[0,100]
5/2+	12	[0,100]

Throw a BRICK at it 

- Publicly available Python code

  https://github.com/odell/brick
- Available on PyPI
- BAND Framework v0.4

  bandframework.github.io
- AZURE2 must be installed
- User specifies R-matrix model & data set in AZURE2
- Specify priors & likelihood

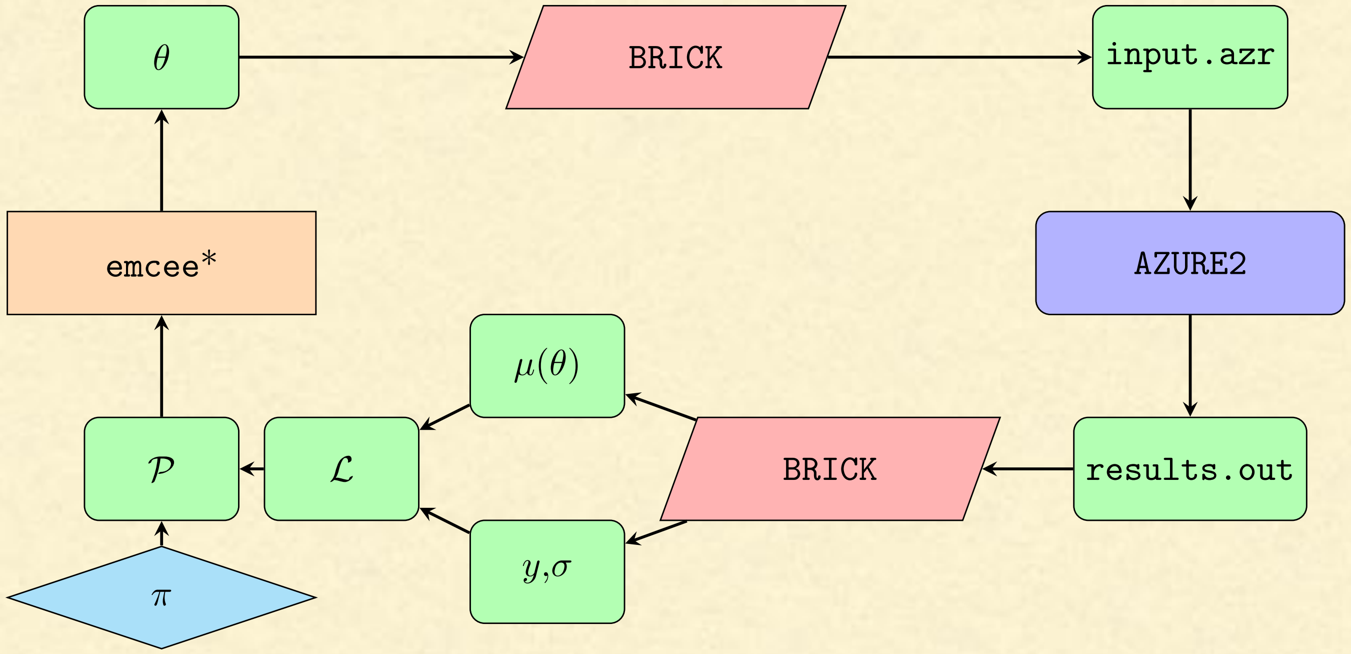

Throw a BRICK at it

- Publicly available Python code
  https://github.com/odell/brick
- Available on PyPI
- BAND Framework v0.4
  bandframework.github.io
- AZURE2 must be installed
- User specifies R-matrix model & data set in AZURE2
- Specify priors & likelihood

$$\mathscr{L} \propto \prod_{\alpha=1}^{N_{\text{sets}}} \prod_{j=1}^{N_\alpha} \exp\left(-\frac{(y_{j\alpha} - f_\alpha \mu(x_{j\alpha}; \theta_R))^2}{2\sigma_{j,\alpha}^2} \right)$$

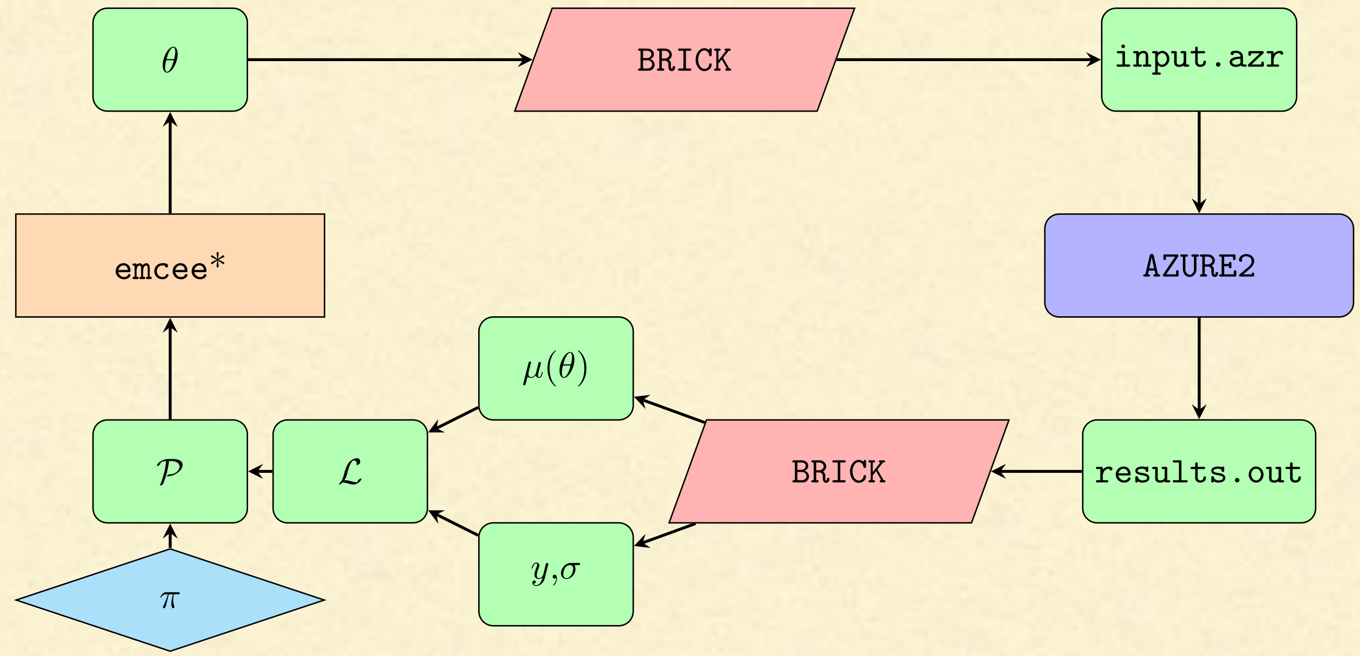

Throw a BRICK at it

- Publicly available Python code
  https://github.com/odell/brick
- Available on PyPI
- BAND Framework v0.4
  bandframework.github.io
- AZURE2 must be installed
- User specifies R-matrix model & data set in AZURE2
- Specify priors & likelihood

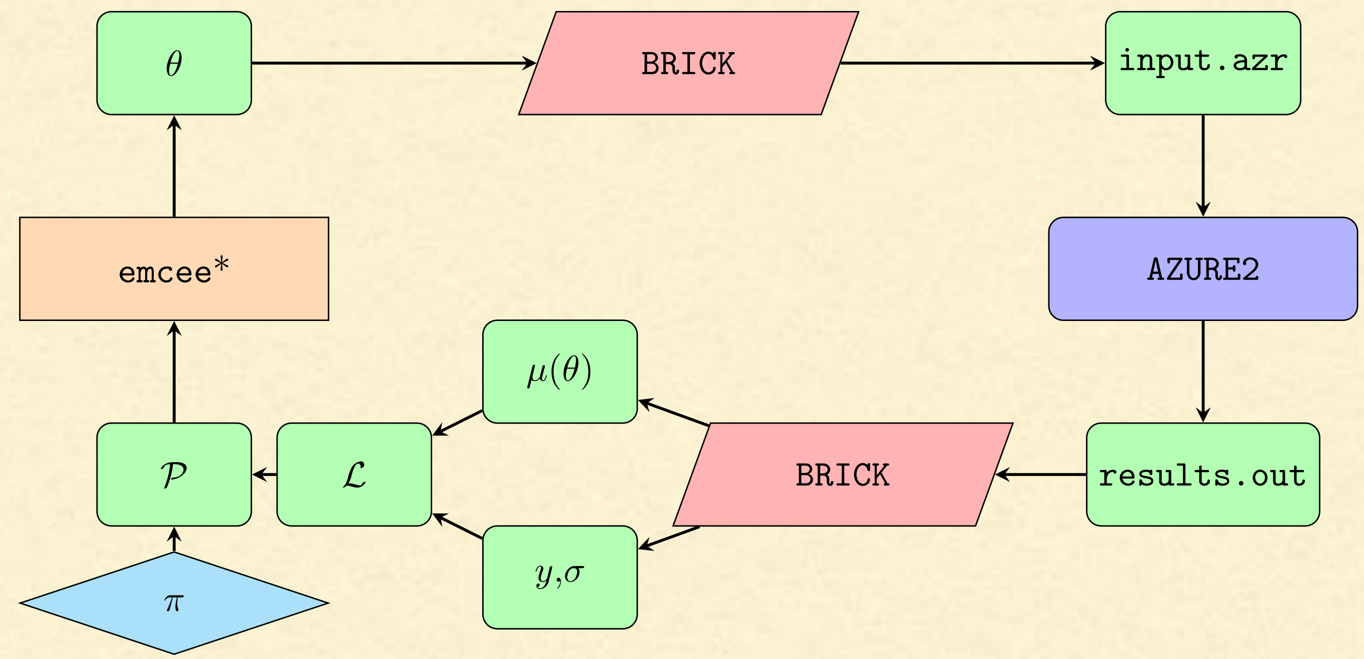

$$\mathscr{L} \propto \prod_{\alpha=1}^{N_{\text{sets}}} \prod_{j=1}^{N_\alpha} \exp\left(-\frac{(y_{j\alpha} - f_\alpha \mu(x_{j\alpha};\theta_R))^2}{2\sigma_{j,\alpha}^2} \right)$$

Data

Throw a BRICK at it 

Bayesian Analysis of Nuclear Dynamics

- Publicly available Python code
  https://github.com/odell/brick
- Available on PyPI
- BAND Framework v0.4
  bandframework.github.io
- AZURE2 must be installed
- User specifies R-matrix model & data set in AZURE2
- Specify priors & likelihood

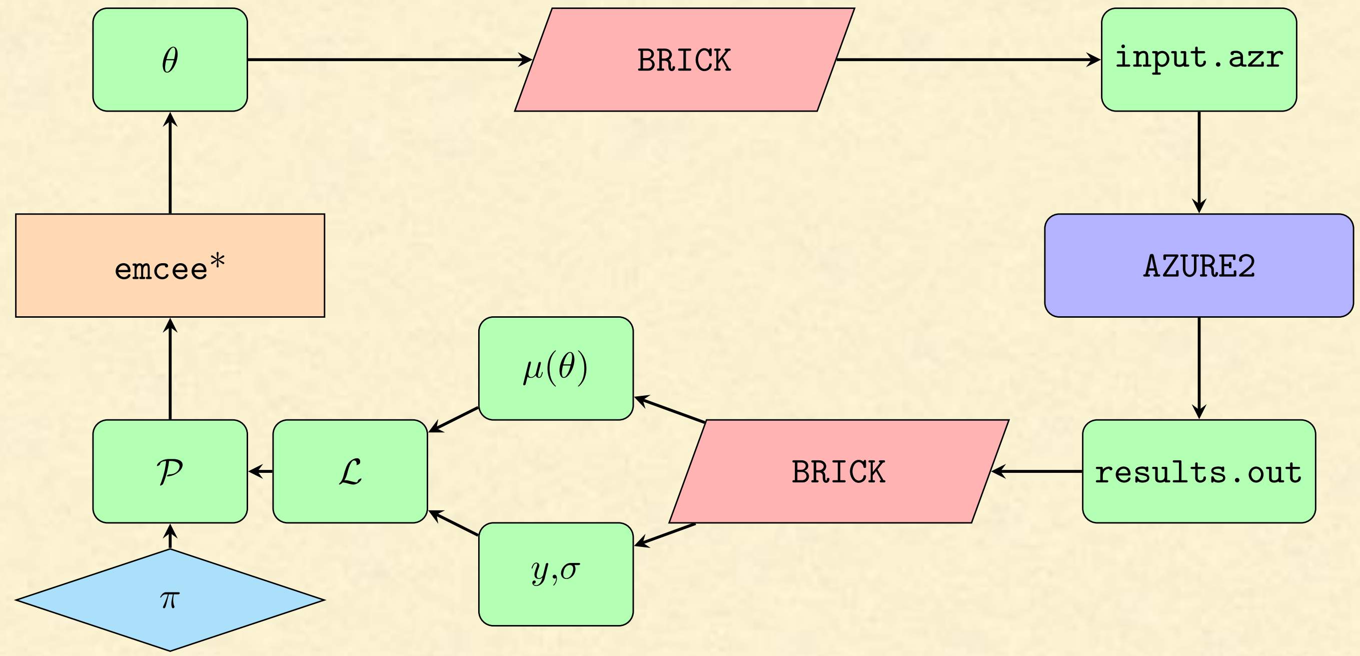

$$\mathscr{L} \propto \prod_{\alpha=1}^{N_{\text{sets}}} \prod_{j=1}^{N_\alpha} \exp\left(- \frac{(y_{j\alpha} - f_\alpha \mu(x_{j\alpha}; \theta_R))^2}{2\sigma_{j,\alpha}^2} \right)$$

R-matrix number

Data

Throw a BRICK at it

- Publicly available Python code

  https://github.com/odell/brick
- Available on PyPI
- BAND Framework v0.4

  bandframework.github.io
- AZURE2 must be installed
- User specifies R-matrix model & data set in AZURE2
- Specify priors & likelihood

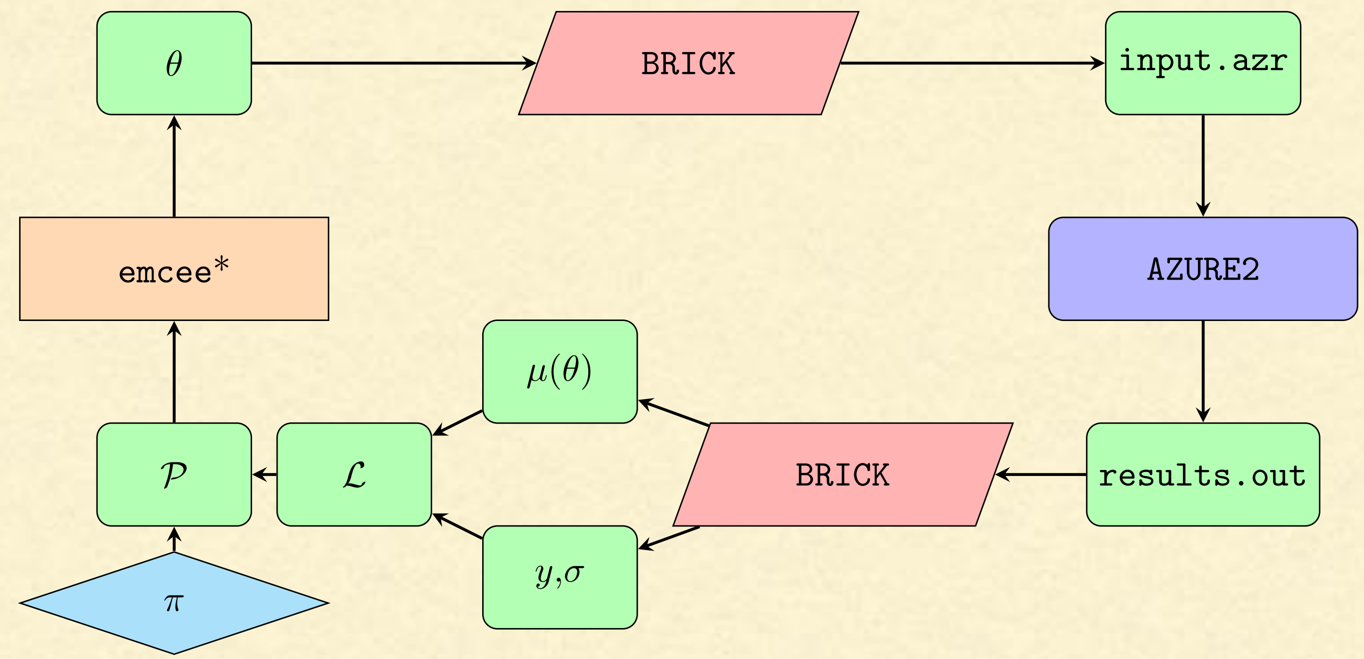

Data normalization

R-matrix number

$$\mathscr{L} \propto \prod_{\alpha=1}^{N_{\text{sets}}} \prod_{j=1}^{N_\alpha} \exp\left(-\frac{(y_{j\alpha} - f_\alpha \mu(x_{j\alpha}; \theta_R))^2}{2\sigma_{j,\alpha}^2} \right)$$

Data

The benefits of Bayesian parameter estimation

The benefits of Bayesian parameter estimation

- Straightforward to introduce additional nuisance parameters to model experimental imperfections. Marginalizing over them includes impact of those imperfections on parameters and evaluated quantities

- Access to full multi-dimensional posterior for parameters, not just properties around a (local) minimum

- With samples of R-matrix parameters in hand, straightforward to evaluate any observable we want for all those samples⟹error propagation is a snap!

$$\mathrm{pr}(S(E_0)\,|\,D, I) = \int d\vec{\theta}\,\delta(S(E_0) - S_{\mathrm{R-matrix}}(E_0;\vec{\theta}))\,\mathrm{pr}(\vec{\theta}\,|\,D, I)$$

- Not just experimental imperfections either! Theory imperfections can be accounted for too

Modeling of normalization uncertainties

- Analysis includes common-mode errors for all data sets, implemented by factor f_α to avoid d'Agostini bias
- For SONIK data set this normalization factor is assigned for each beam energy
- Almost all normalizations come out inside quoted CMEs, all are within 2*CME, apart from LUNA in CSB analysis
- "Dialogue with the data"

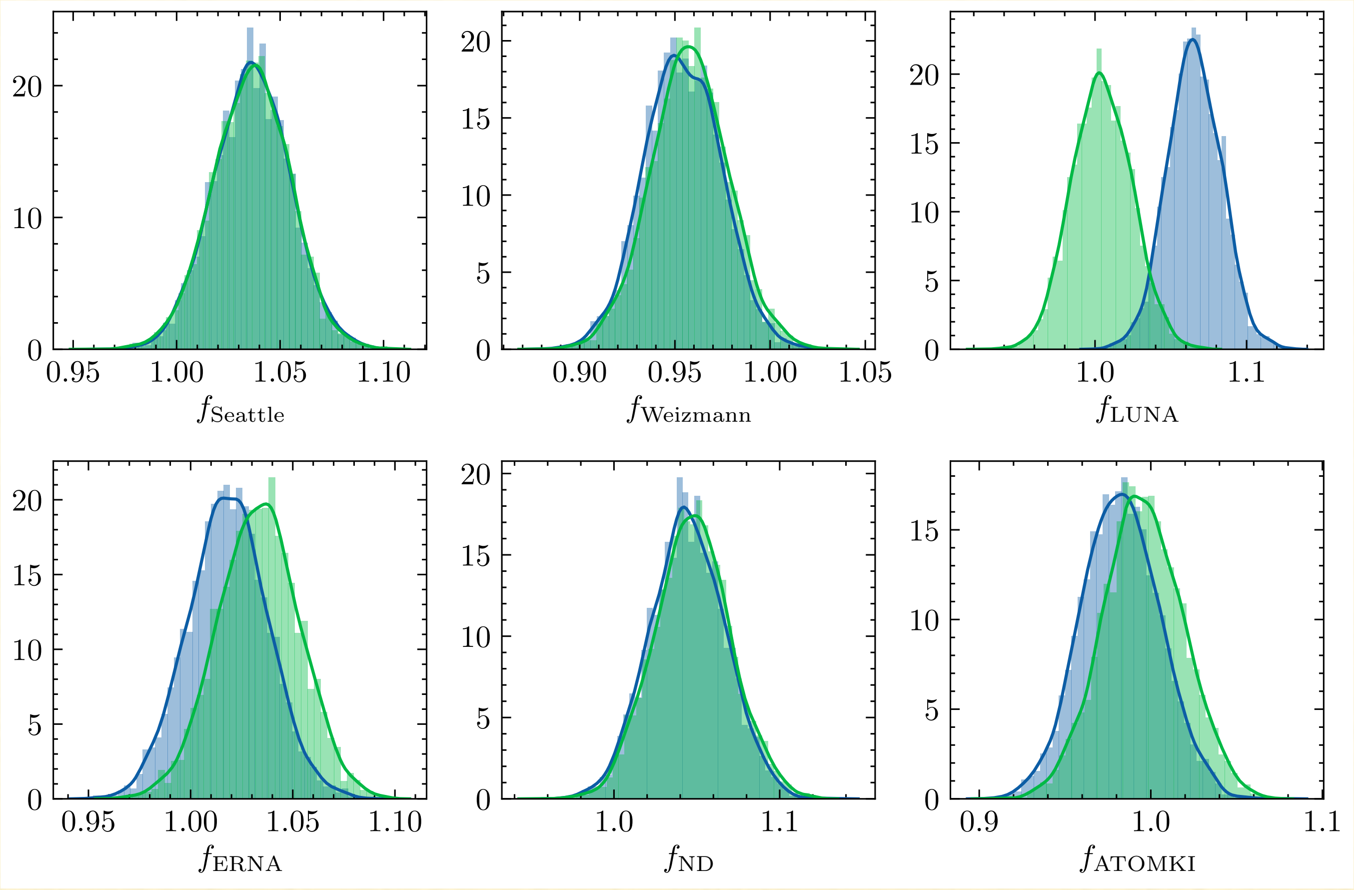

CS

CSB

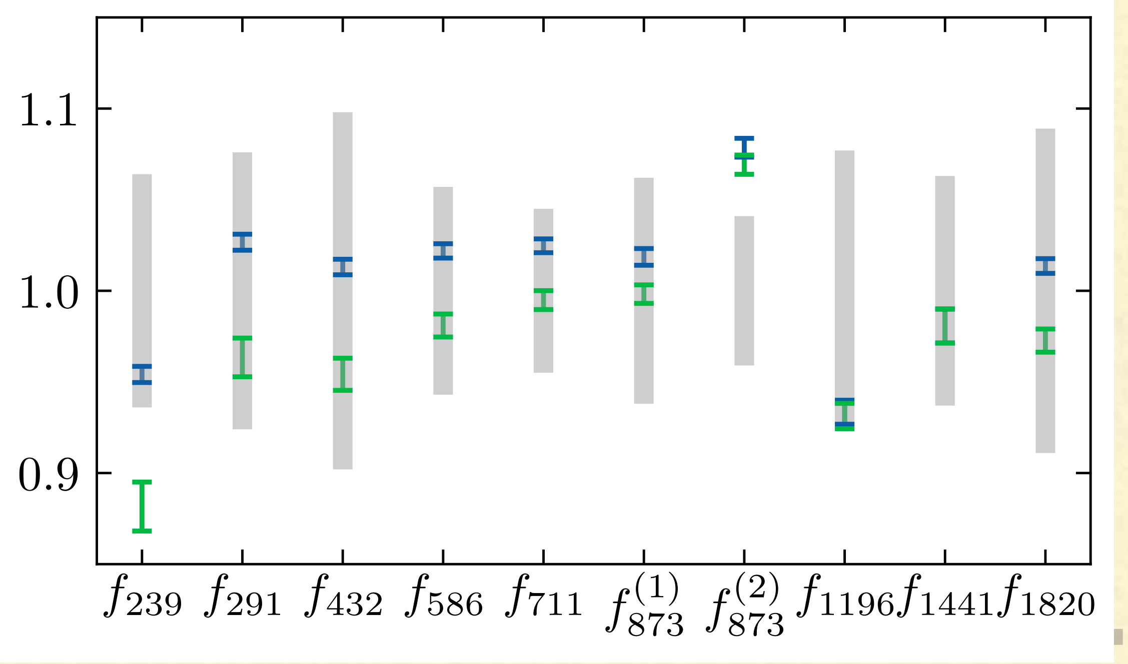

More sophisticated normalization modeling

Paneru, Brune, Connelly, Odell, ..., DP, et al., PRC (to appear)

More sophisticated normalization modeling

Paneru, Brune, Connelly, Odell, ..., DP, et al., PRC (to appear)

- After this slide I'll only show results from that 2022 Frontiers paper's analysis of data, but first I want to mention something more sophisticated that was done to model the SONIK systematics

More sophisticated normalization modeling

Paneru, Brune, Connelly, Odell, ..., DP, et al., PRC (to appear)

- After this slide I'll only show results from that 2022 Frontiers paper's analysis of data, but first I want to mention something more sophisticated that was done to model the SONIK systematics
- Consider not just beam normalization uncertainty, but also uncertainty due to acceptance (aperture variation) of each of 27 detectors

More sophisticated normalization modeling

Paneru, Brune, Connelly, Odell, ..., DP, et al., PRC (to appear)

- After this slide I'll only show results from that 2022 Frontiers paper's analysis of data, but first I want to mention something more sophisticated that was done to model the SONIK systematics

- Consider not just beam normalization uncertainty, but also uncertainty due to acceptance (aperture variation) of each of 27 detectors

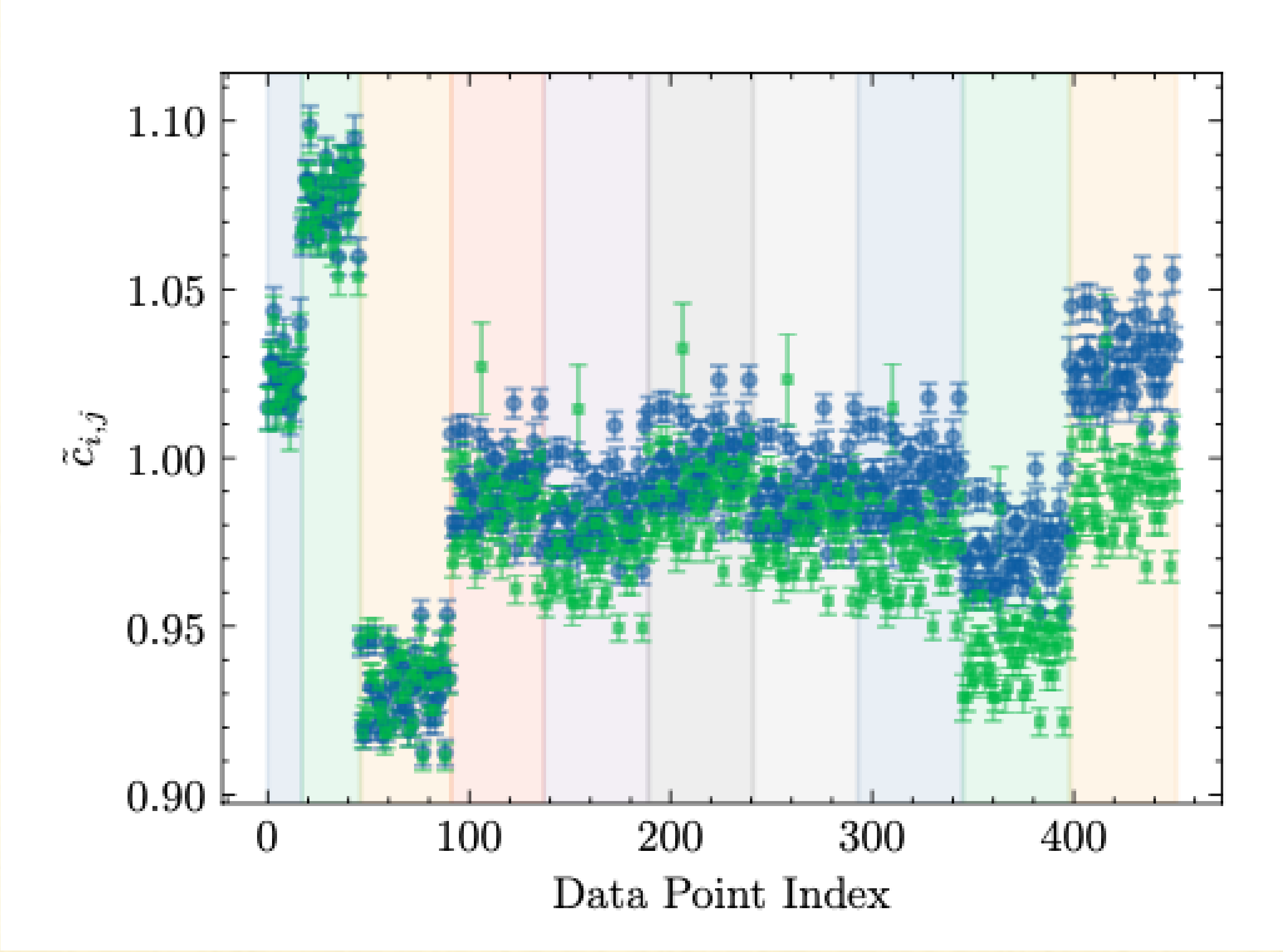

$$y_{\rm exp} = f_{\rm SONIK} f_E f_{\rm det} y_{\rm R} + \delta y_{\rm exp}$$

$$\tilde{c}_{i,j} = f_E f_{\rm det}$$

Green: R-matrix
Blue: EFT

Beam energy shift

Beam energy shift

- Shift energy of Barnard data set by a constant to account for possible miscalibration of beam energy: $E \to E + \Delta$. Prior a Gaussian with standard deviation 40 keV←information in paper

$$\mathscr{L} \propto \prod_{\alpha=1}^{N_{\rm sets}} \prod_{j=1}^{N_\alpha} \exp\left(-\frac{(y_{j\alpha} - f_\alpha \mu(E_{j\alpha} + \Delta, \phi_{j\alpha}; \theta_R))^2}{2\sigma_{j,\alpha}^2}\right)$$

Beam energy shift

- Shift energy of Barnard data set by a constant to account for possible miscalibration of beam energy: $E \to E + \Delta$. Prior a Gaussian with standard deviation 40 keV ← information in paper

$$\mathscr{L} \propto \prod_{\alpha=1}^{N_{\text{sets}}} \prod_{j=1}^{N_\alpha} \exp\left(-\frac{(y_{j\alpha} - f_\alpha \mu(E_{j\alpha} + \Delta, \phi_{j\alpha}; \theta_R))^2}{2\sigma_{j,\alpha}^2} \right)$$

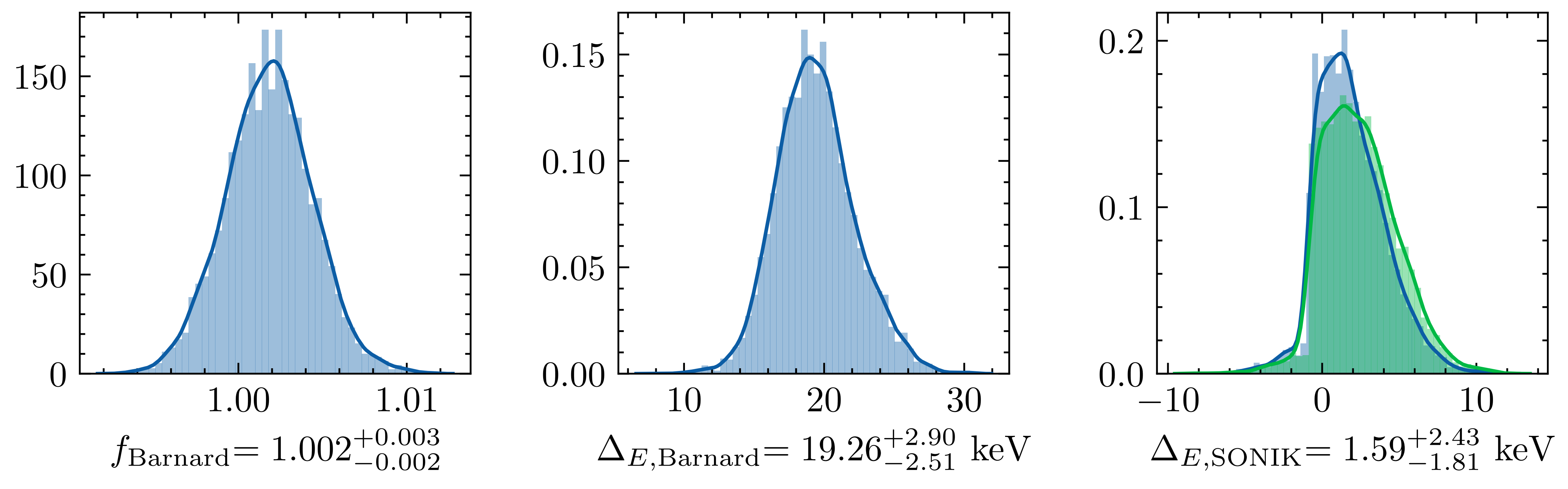

CS

CSB

Beam energy shift

- Shift energy of Barnard data set by a constant to account for possible miscalibration of beam energy: $E \to E + \Delta$. Prior a Gaussian with standard deviation 40 keV ← information in paper

$$\mathscr{L} \propto \prod_{\alpha=1}^{N_{\mathrm{sets}}} \prod_{j=1}^{N_\alpha} \exp\left(- \frac{(y_{j\alpha} - f_\alpha \mu(E_{j\alpha} + \Delta, \phi_{j\alpha}; \theta_R))^2}{2\sigma_{j,\alpha}^2} \right)$$

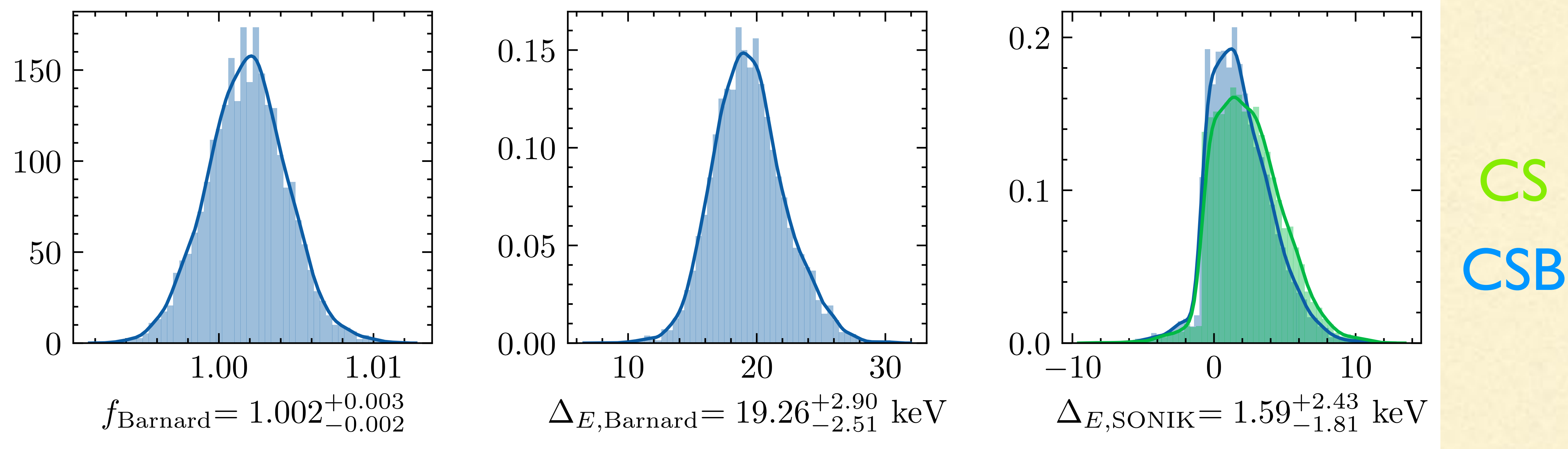

- No significant change in $\vec{\theta}_{\mathrm{Barnard}}$ due to this though

Posteriors for R-matrix parameters

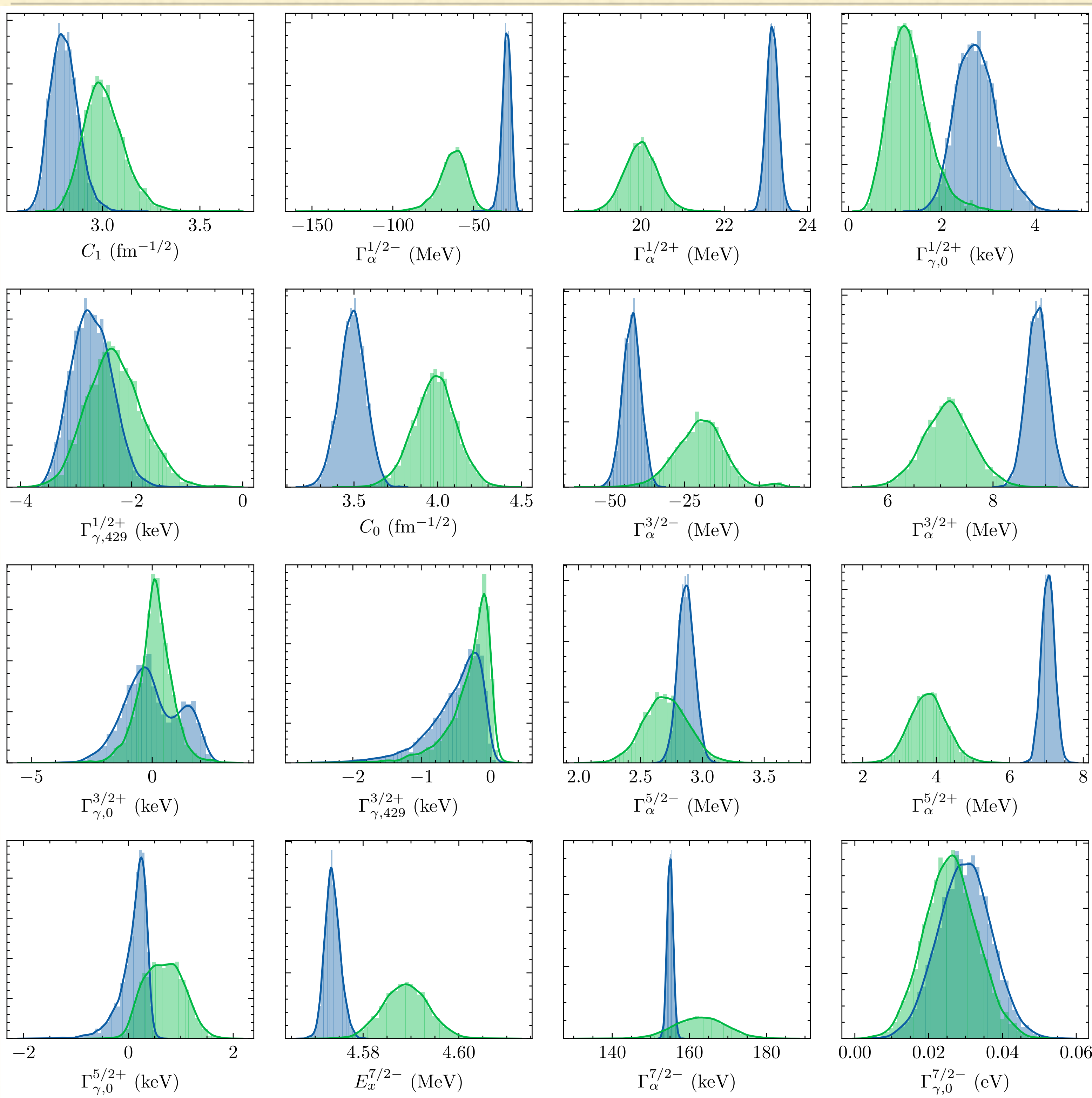

Capture + SONIK

Capture + SONIK + Barnard

Posteriors for R-matrix parameters

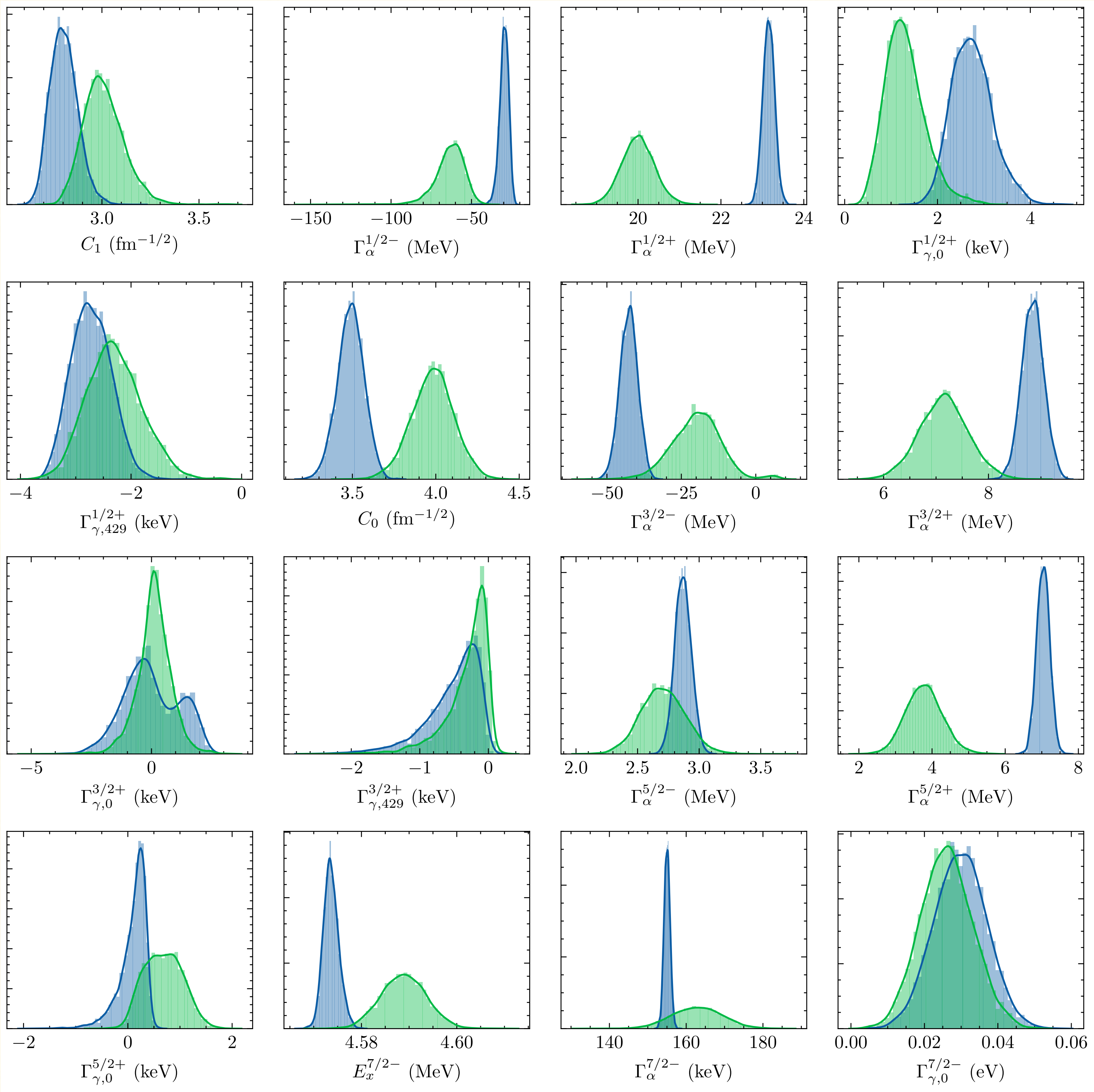

Capture + SONIK

Capture + SONIK + Barnard

Notable points:

- ANCs
- $\Gamma_\alpha^{7/2-}$
- Non-Gaussianity

Posteriors for R-matrix parameters

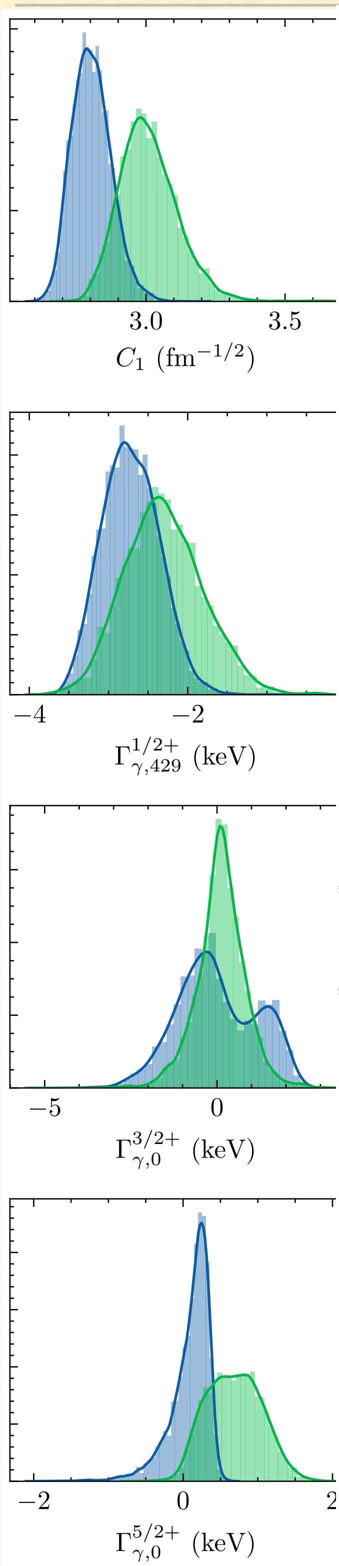

Access to all covariance information

re + SONIK

SONIK + Barnard

ble points:

Cs

2−

n-Gaussianity

But why didn’t you just use MINUIT?

But why didn't you just use MINUIT?

- Diagnose non-Gaussianity

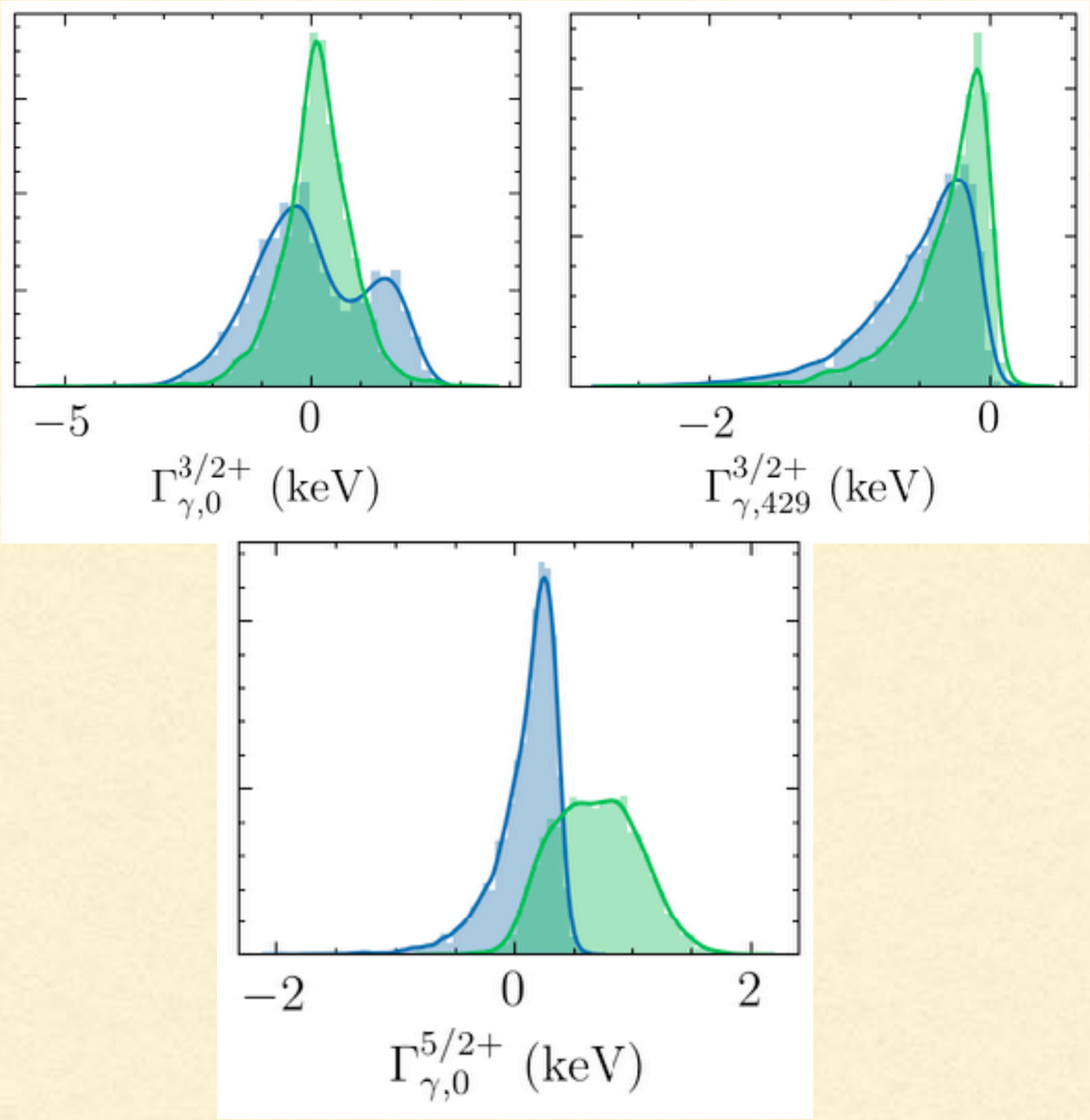

But why didn't you just use MINUIT?

- Diagnose non-Gaussianity
- Very clear when posterior "returns the prior" for a particular parameter and so that parameter is not really needed for the fit.

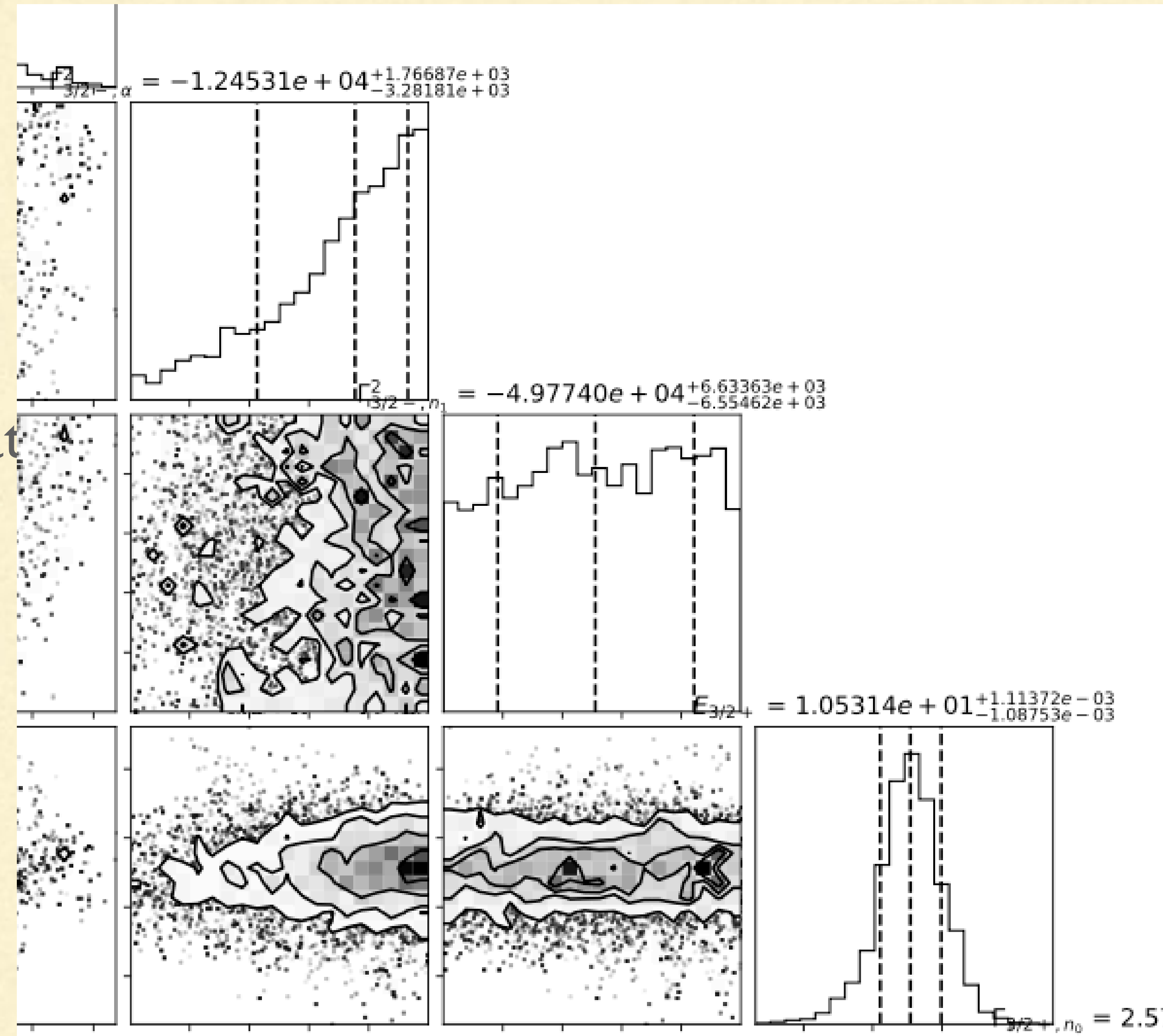

^{13}C(α,n), courtesy James deBoer

But why didn't you just use MINUIT?

- Diagnose non-Gaussianity
- Very clear when posterior "returns the prior" for a particular parameter and so that parameter is not really needed for the fit.
- (Note that it's also clear when prior is affecting shape of posterior.)

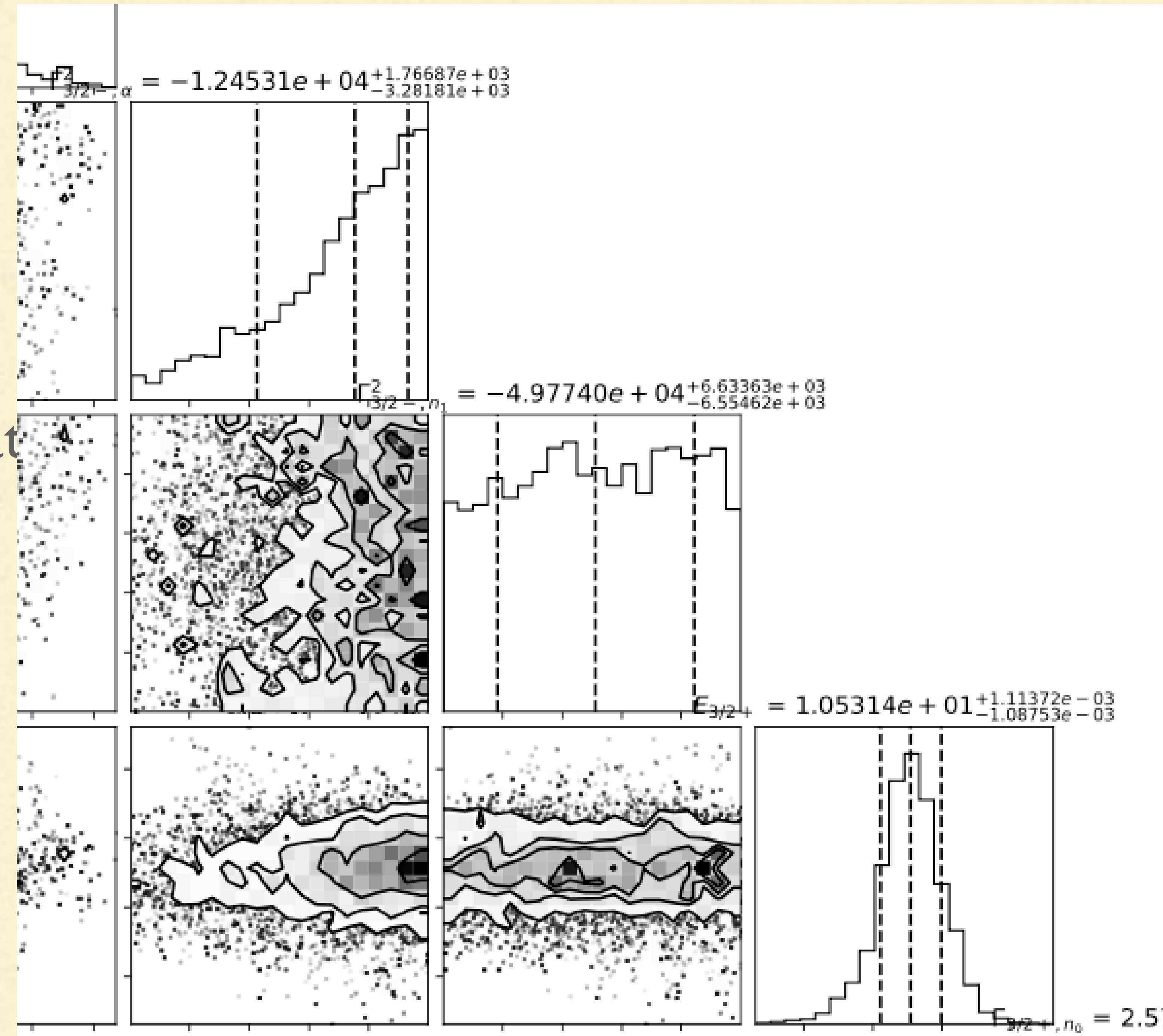

^{13}C(α,n), courtesy James deBoer

But why didn't you just use MINUIT?

- Diagnose non-Gaussianity
- Very clear when posterior "returns the prior" for a particular parameter and so that parameter is not really needed for the fit.
- (Note that it's also clear when prior is affecting shape of posterior.)
- Also, error propagation….

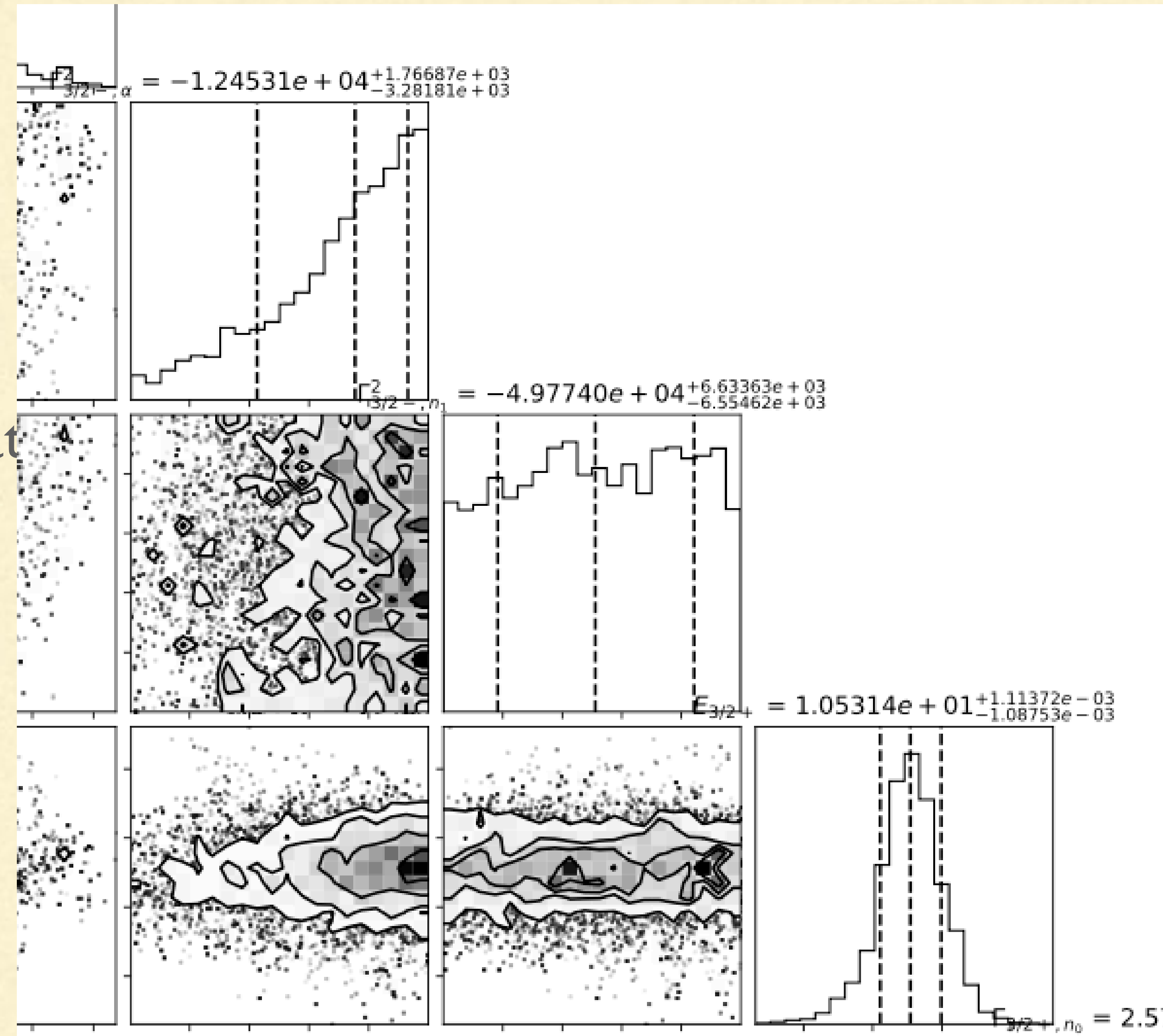

^{13}C(α,n), courtesy James deBoer

Speaking of which: SONIK data looks good

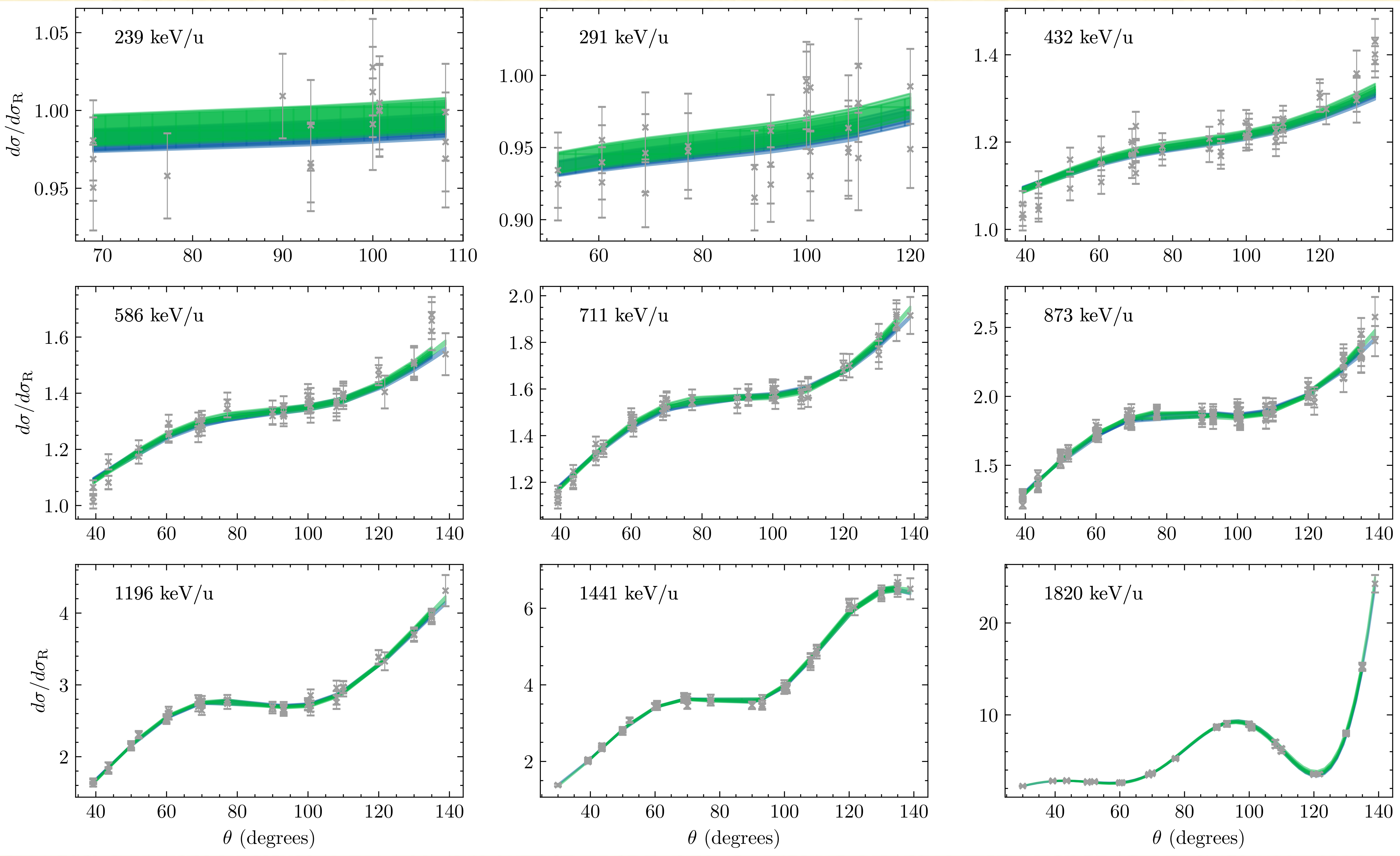

What about S-factor at solar energies?

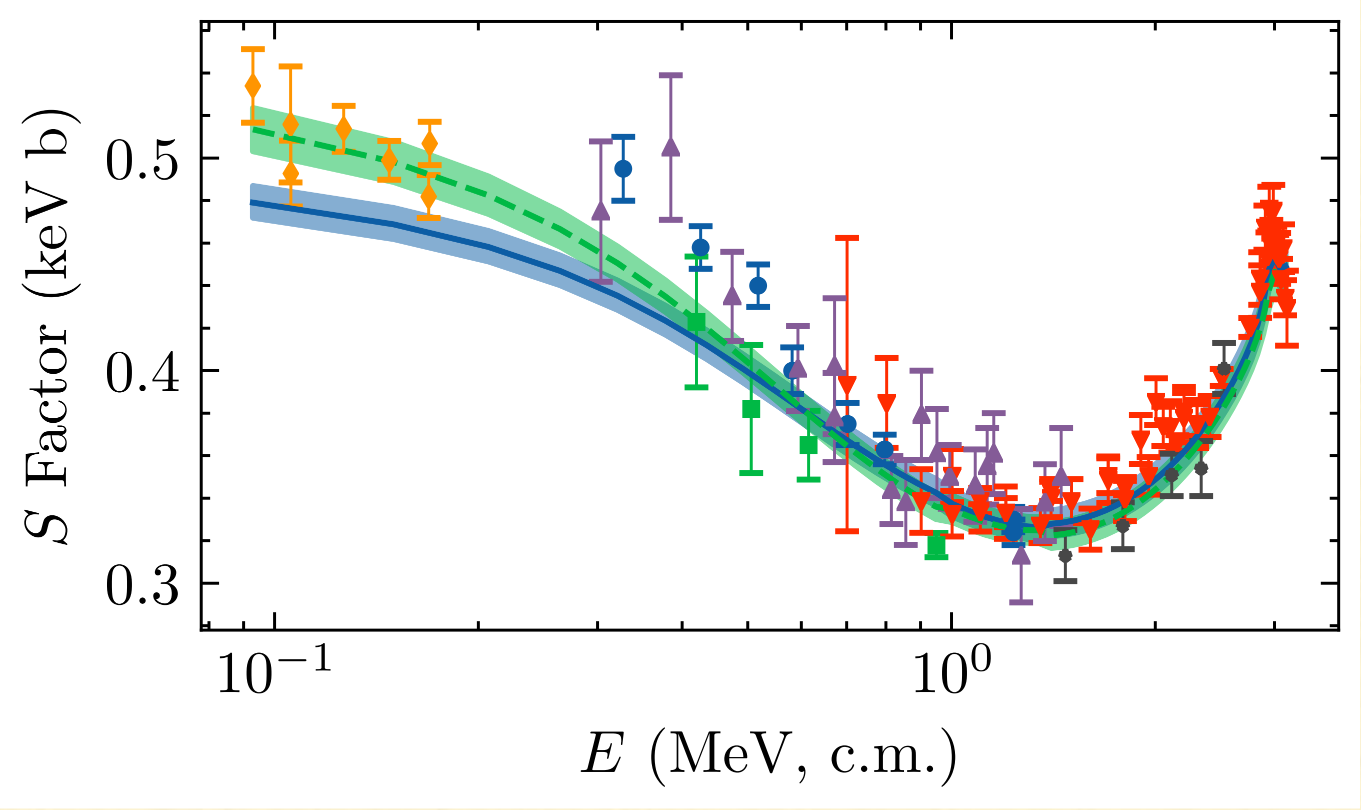

What about S-factor at solar energies?

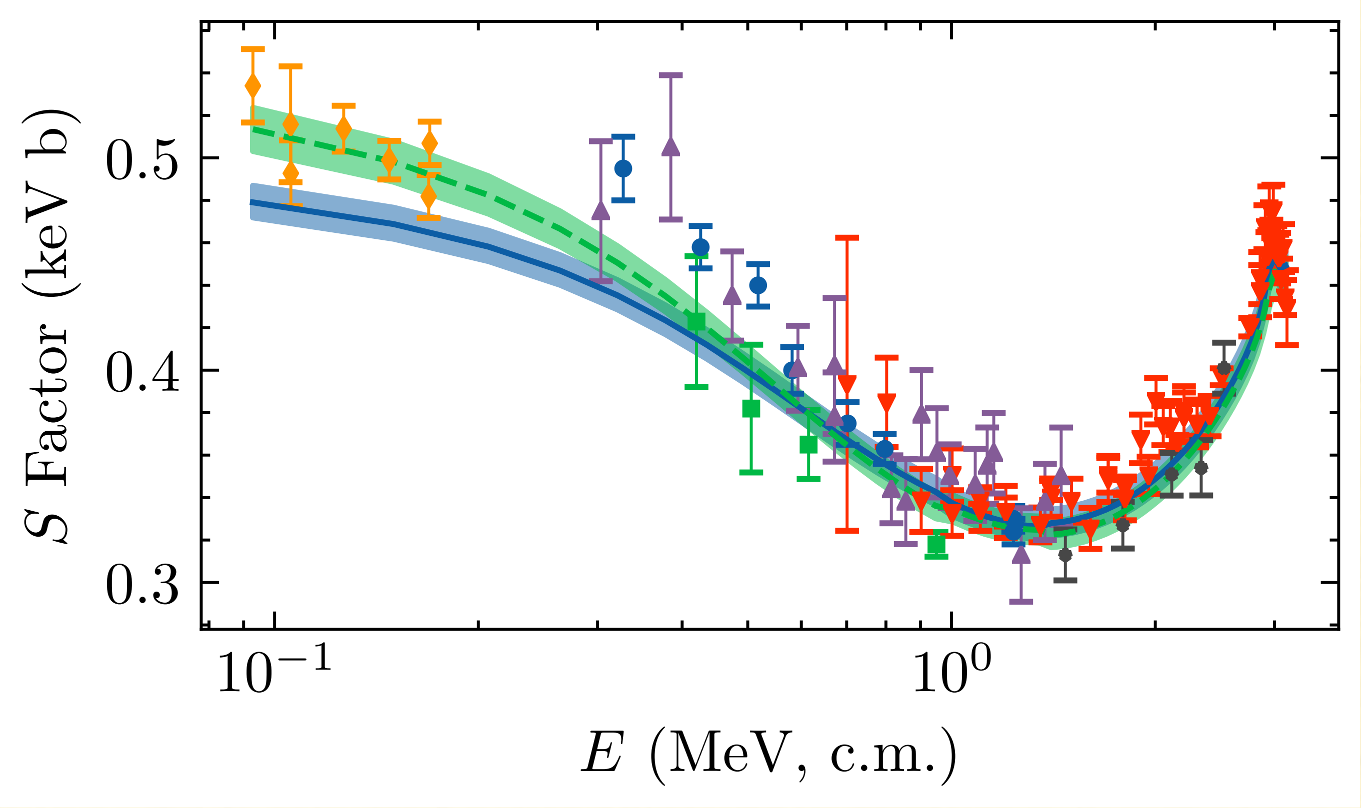

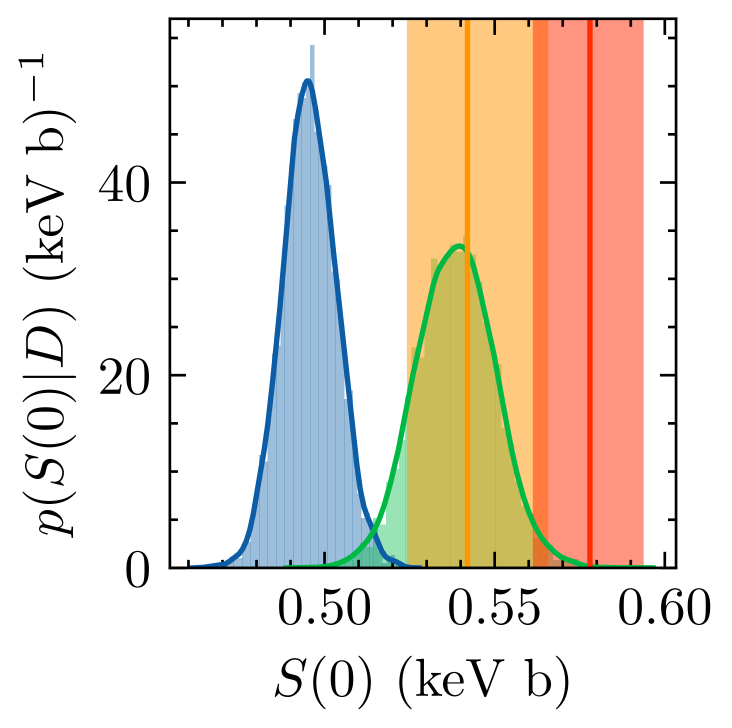

- Blue: CSB
- Green: CS
- Orange: de Boer et al.
- Red: Zhang, Nollett, DP

What about S-factor at solar energies?

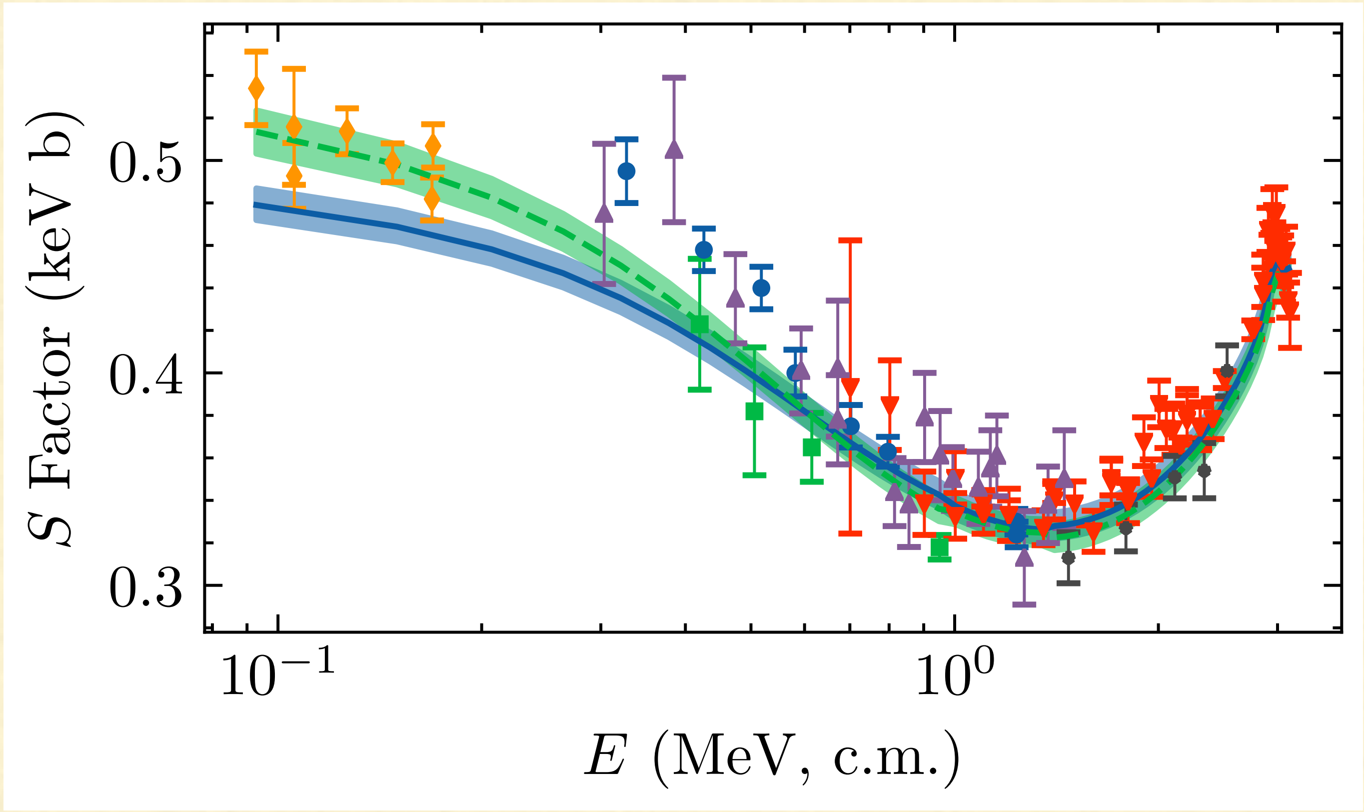

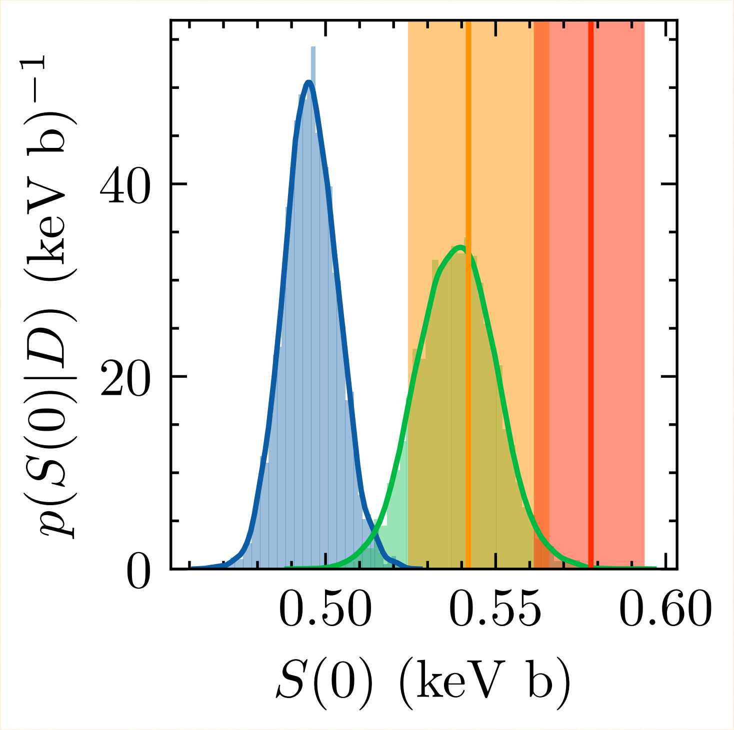

- Blue: CSB
- Green: CS
- Orange: de Boer et al.
- Red: Zhang, Nollett, DP

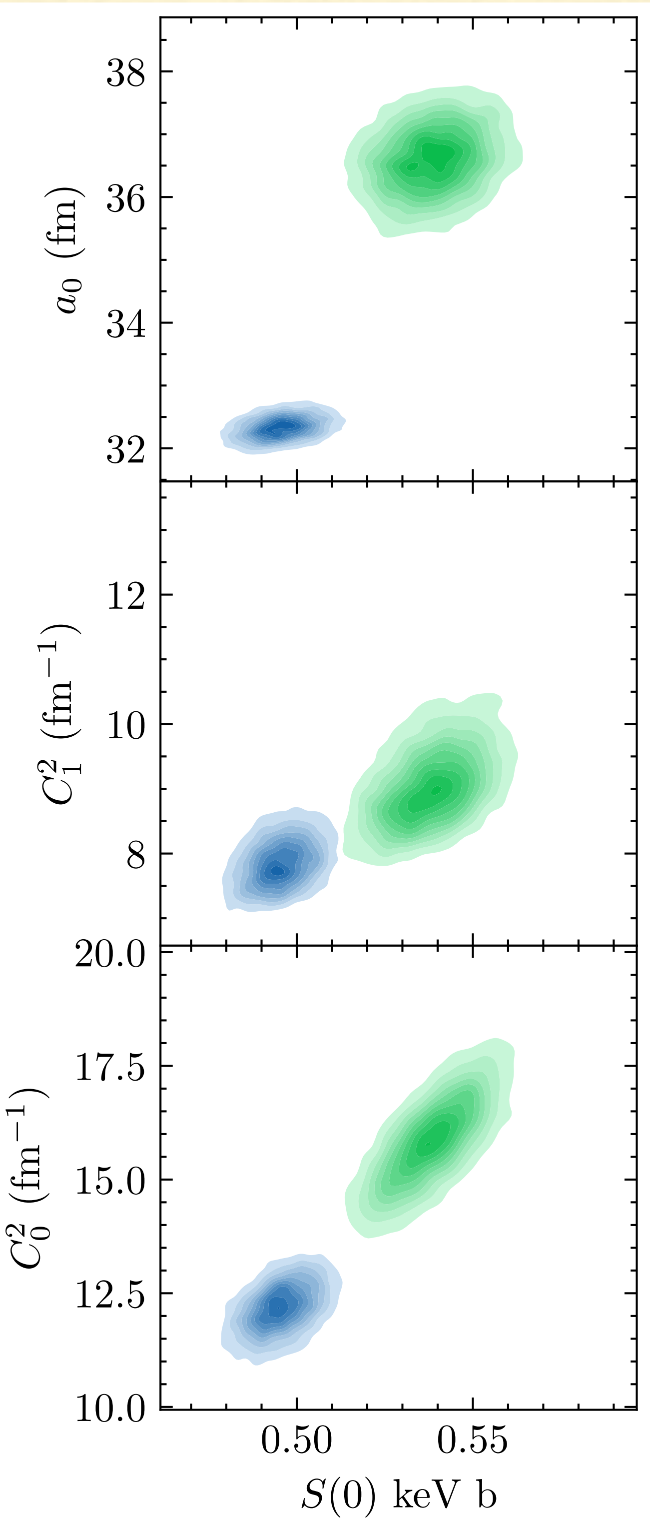

Halo EFT

Bertulani, Hammer, van Kolck, NPA (2003);
Bedaque, Hammer, van Kolck, PLB (2003);
Reviews: Hammer, Ji, DP, J. Phys. G 44, 103002 (2017);

$\lambda \gg R_{core}$; $\lambda \lesssim R_{halo}$

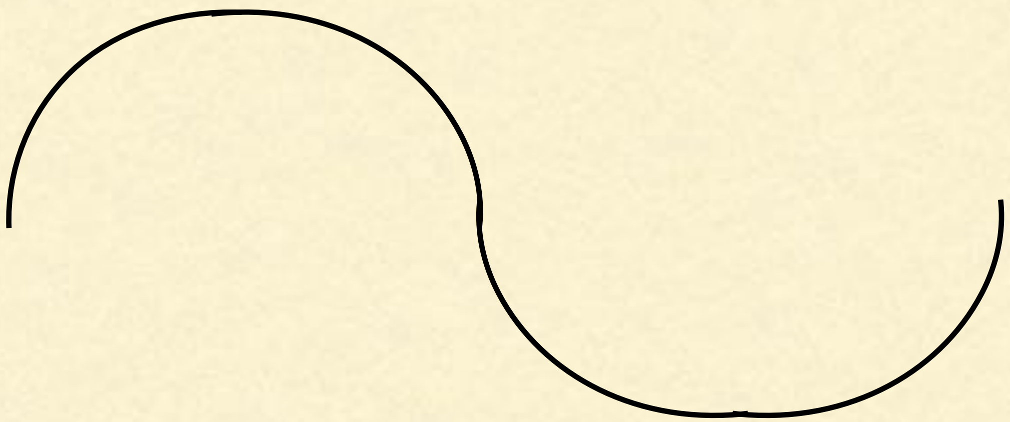

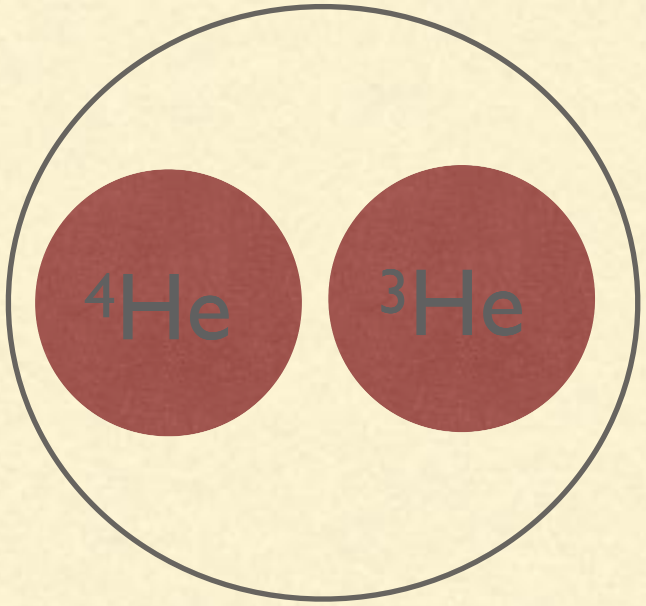

Halo EFT

Bertulani, Hammer, van Kolck, NPA (2003);
Bedaque, Hammer, van Kolck, PLB (2003);
Reviews: Hammer, Ji, DP, J. Phys. G 44, 103002 (2017);

$\lambda \gg R_{core}$; $\lambda \lesssim R_{halo}$

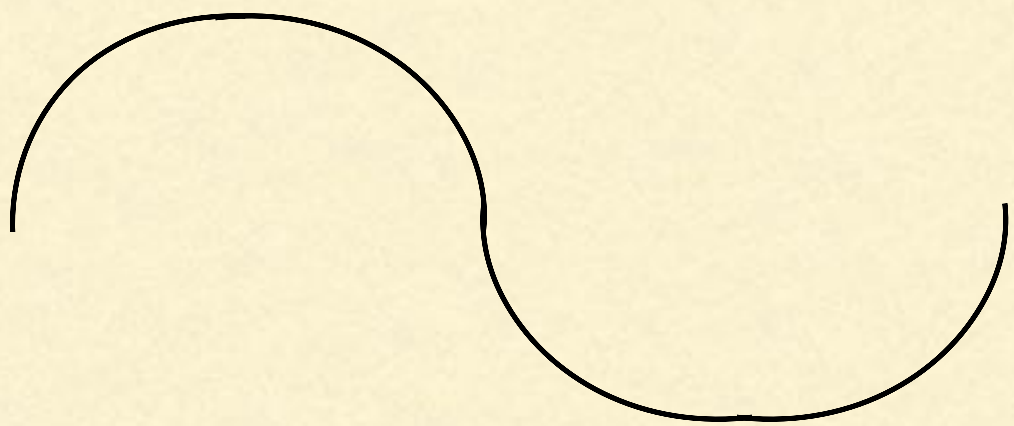

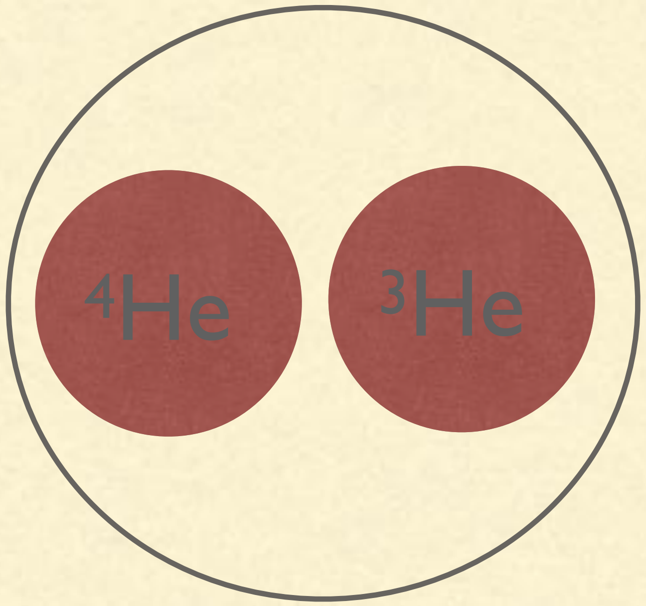

- Consider photo disintegration of ^{7}Be at long wavelength
- Define $R_{halo}=\langle r^2\rangle^{1/2}$. Seek EFT expansion in R_{core}/R_{halo}. Valid for $\lambda \lesssim R_{halo}$
- Here $R \equiv R_{core} \sim 1.5$ fm. So this approach should be valid up to momenta of order 100 MeV
- Updates and systematizes cluster models

p-wave bound states and capture thereto

Hammer & DP, NPA (2011)

- At LO p-wave 1n halo described solely by its ANC and binding energy

$$u_1(r) = A_1 \exp(-\gamma_1 r)\left(1 + \frac{1}{\gamma_1 r}\right) \qquad \gamma_1 = \sqrt{2m_R B}$$

- Capture to the p-wave state proceeds via the one-body E1 operator: "external direct capture"

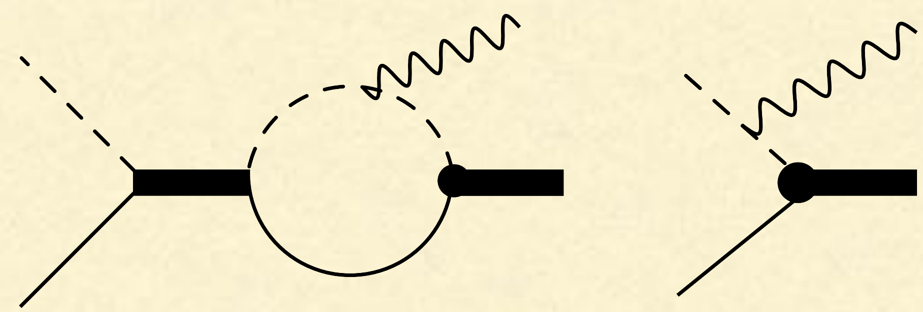

$$\text{E1} \propto \int dr\, u_1(r) r(\cos(kr) + \sin(kr)\ \cot\delta);\, k\cot\delta \text{ from ERE}$$

- NLO: piece of the amplitude representing capture at short distances, represented by a contact operator⇒there is an LEC that must be fit

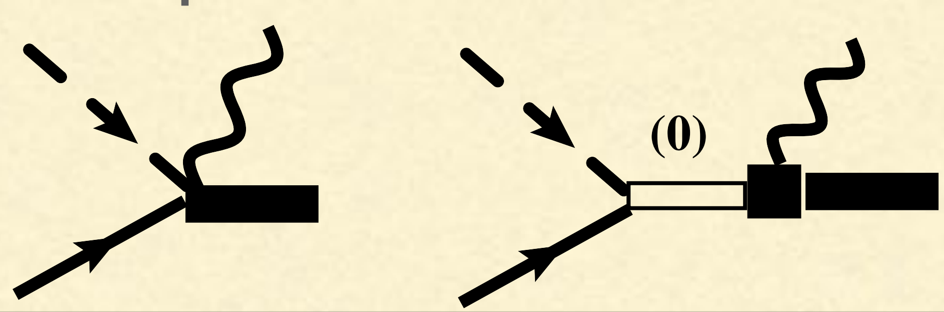

$^3He + {}^4He \to {}^7Be + \gamma_{E1}$ at LO in Halo EFT

Zhang, Nollett, DP, JPG (2019), cf. Rupak, Higa, Vaghani, EPJA (2018)

- In this system $R_{core} \sim 1.5$ fm, $R_{halo} \sim 3$ fm

^{3}He + ^{4}He→^{7}Be + γ_{E1} at LO in Halo EFT

Zhang, Nollett, DP, JPG (2019), cf. Rupak, Higa, Vaghani, EPJA (2018)

- In this system R_{core}~1.5 fm, R_{halo} ~3 fm
- Also need to include Coulomb interactions non-perturbatively: $k_C=Q_cQ_n\alpha_{EM}M_R$=17 MeV; a~10s of fm, both ~R_{halo}

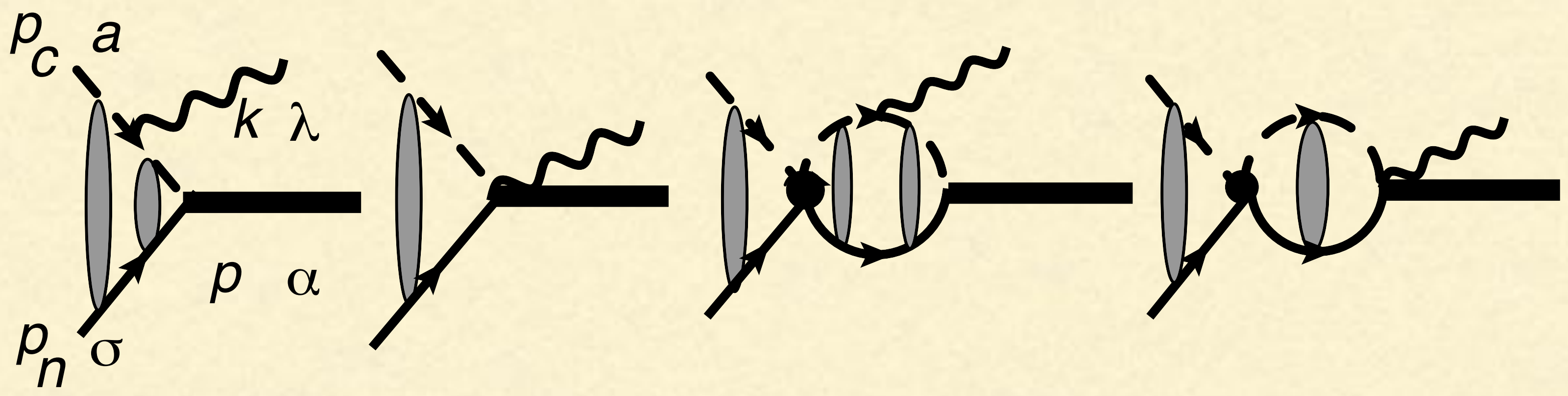

^{3}He + ^{4}He→^{7}Be + γ_{E1} at LO in Halo EFT

Zhang, Nollett, DP, JPG (2019), cf. Rupak, Higa, Vaghani, EPJA (2018)

- In this system R_{core}~1.5 fm, R_{halo} ~3 fm
- Also need to include Coulomb interactions non-perturbatively: $k_C=Q_cQ_n\alpha_{EM}M_R$=17 MeV; a~10s of fm, both ~R_{halo}

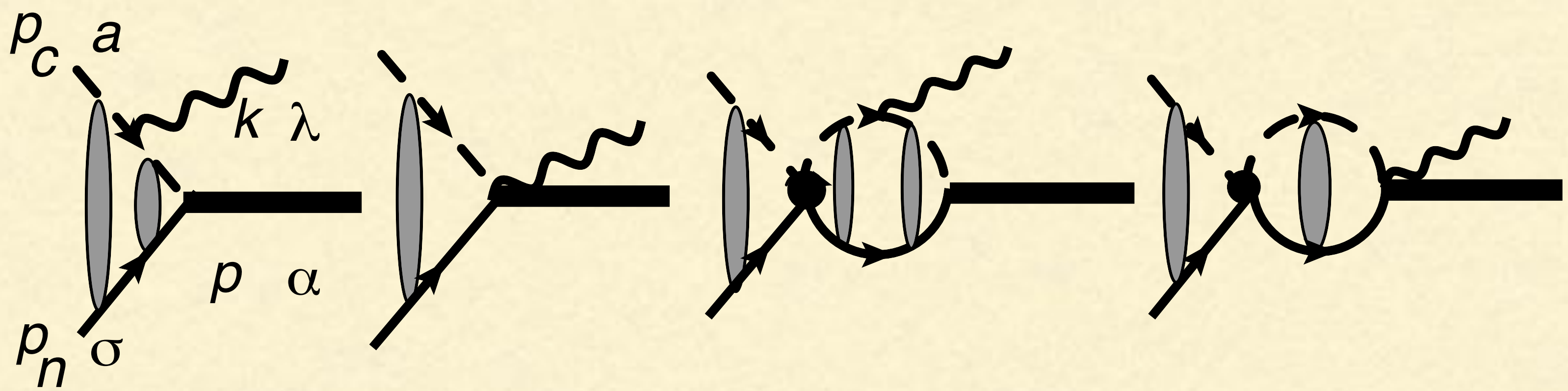

- Scattering wave functions are linear combinations of Coulomb wave functions F_0 and G_0. Bound state wave function=the appropriate Whittaker function.

$^3He + {}^4He \rightarrow {}^7Be + \gamma_{E1}$ at LO in Halo EFT

Zhang, Nollett, DP, JPG (2019), cf. Rupak, Higa, Vaghani, EPJA (2018)

- In this system $R_{core} \sim 1.5$ fm, $R_{halo} \sim 3$ fm
- Also need to include Coulomb interactions non-perturbatively: $k_C = Q_c Q_n \alpha_{EM} M_R = 17$ MeV; a~10s of fm, both ~R_{halo}

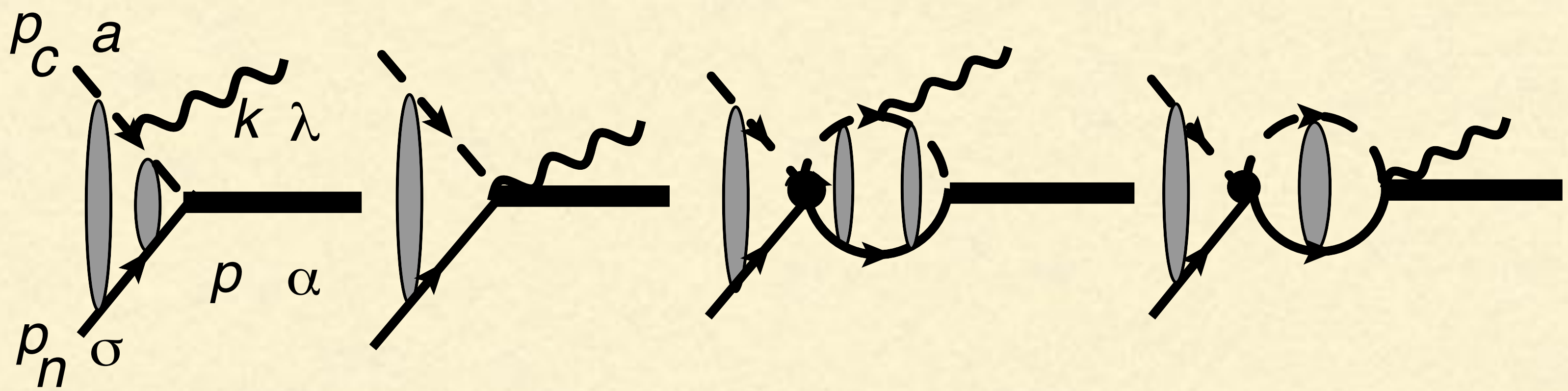

- Scattering wave functions are linear combinations of Coulomb wave functions F_0 and G_0. Bound state wave function=the appropriate Whittaker function.

$$S(E) = \frac{e^{2\pi\eta}}{e^{2\pi\eta}-1}\frac{8\pi}{9}(eZ_{eff})^2 k_C \omega^3 C^2 \left[|\mathcal{S}_{EC}(E;\delta(E))|^2 + |\mathcal{D}(E)|^2 \right]$$

$^3He + {}^4He \to {}^7Be + \gamma_{E1}$ at LO in Halo EFT

Zhang, Nollett, DP, JPG (2019), cf. Rupak, Higa, Vaghani, EPJA (2018)

- In this system $R_{core} \sim 1.5$ fm, $R_{halo} \sim 3$ fm
- Also need to include Coulomb interactions non-perturbatively: $k_C = Q_c Q_n \alpha_{EM} M_R = 17$ MeV; $a \sim 10$s of fm, both $\sim R_{halo}$

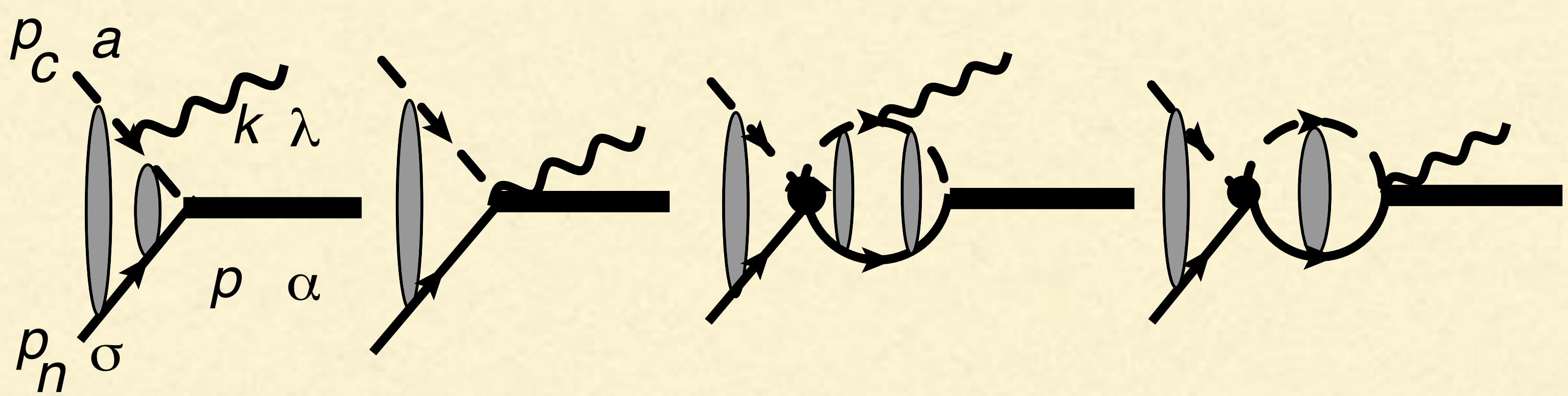

- Scattering wave functions are linear combinations of Coulomb wave functions F_0 and G_0. Bound state wave function=the appropriate Whittaker function.

$$S(E) = \frac{e^{2\pi\eta}}{e^{2\pi\eta}-1}\frac{8\pi}{9}(eZ_{eff})^2 k_C \omega^3 C^2 \left[|\mathcal{S}_{EC}(E;\delta(E))|^2 + |\mathcal{D}(E)|^2 \right]$$

- Can also predict capture to the excited $1/2^-$ in ^7Be

Three parameters at leading order

Additional ingredients at NLO

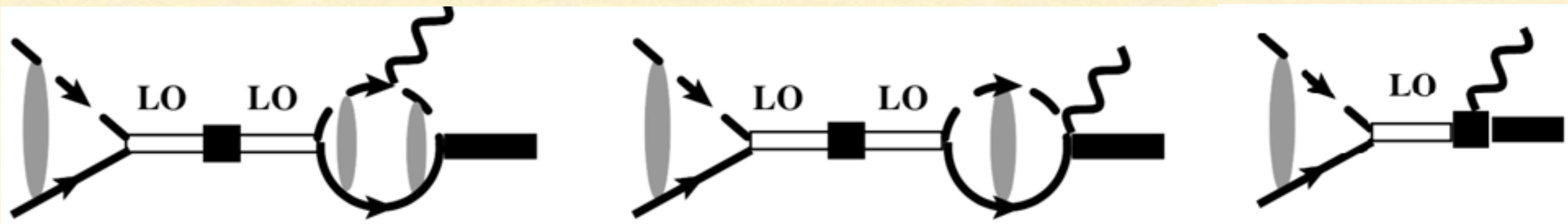

$$S(E) = \frac{e^{2\pi\eta}}{e^{2\pi\eta}-1}\frac{8\pi}{9}k_C\omega^3C^2\left[\mathcal{S}_{EC}(E;\delta(E)) + \bar{L}\ \mathcal{S}_{SD}(E;\delta(E))\,|^2 + |\mathcal{D}(E)|^2\right]$$

Three more parameters at NLO

- Effective range (can add shape parameter which enters at N^{3}LO)
- LECs associated with contact interaction, $\bar{L}$ and $\bar{L}_*$
- Can also consider contact interaction for D-wave capture, $\bar{L}_D$ (enters at N^{4}LO)

Additional ingredients at NLO

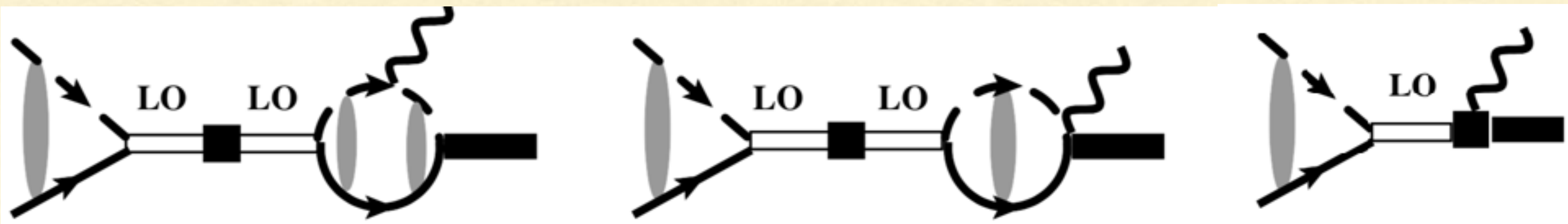

$$S(E) = \frac{e^{2\pi\eta}}{e^{2\pi\eta}-1}\frac{8\pi}{9}k_C\omega^3 C^2\left[\left|\mathcal{S}_{EC}(E;\delta(E)) + \bar{L}\,\mathcal{S}_{SD}(E;\delta(E))\right|^2 + \left|\mathcal{D}(E)\right|^2\right]$$

Three more parameters at NLO

- Effective range (can add shape parameter which enters at N³LO)
- LECs associated with contact interaction, $\bar{L}$ and $\bar{L}_*$
- Can also consider contact interaction for D-wave capture, $\bar{L}_D$ (enters at N⁴LO)

Pick data sets

- 88 S-factor data
  - Seattle (S)
  - Weizmann
  - Luna (L)
  - Erna
  - Notre Dame
  - Atomki

- Plus 34 branching-ratio data

Pick data sets

- 88 S-factor data
    - Seattle (S)
    - Weizmann
    - Luna (L)
    - Erna
    - Notre Dame
    - Atomki
- Plus 34 branching-ratio data

- Specify CMEs
    - S-factor: by set
    - Branching ratio: none

^{3}He(^{4}He,γ) results

Zhang, Nollett, DP, JPG (2019)
cf. Higa, Rupak, Vaghani, EPJA (2018)

^{3}He(^{4}He,γ) results

Zhang, Nollett, DP, JPG (2019)
cf. Higa, Rupak, Vaghani, EPJA (2018)

- E1 external direct capture to a shallow p-wave bound state
- Only one spin channel

$^{3}He(^{4}He,\gamma)$ results

Zhang, Nollett, DP, JPG (2019)
cf. Higa, Rupak, Vaghani, EPJA (2018)

- E1 external direct capture to a shallow p-wave bound state
- Only one spin channel
- Integral is not dominated by as large r as in $^{7}Be(p,\gamma)$
- More sensitivity to ^{3}He-^{4}He scattering parameterization

$^3He(^4He,\gamma)$ results

Zhang, Nollett, DP, JPG (2019)
cf. Higa, Rupak, Vaghani, EPJA (2018)

- E1 external direct capture to a shallow p-wave bound state
- Only one spin channel
- Integral is not dominated by as large r as in $^7Be(p,\gamma)$
- More sensitivity to ^3He-^4He scattering parameterization

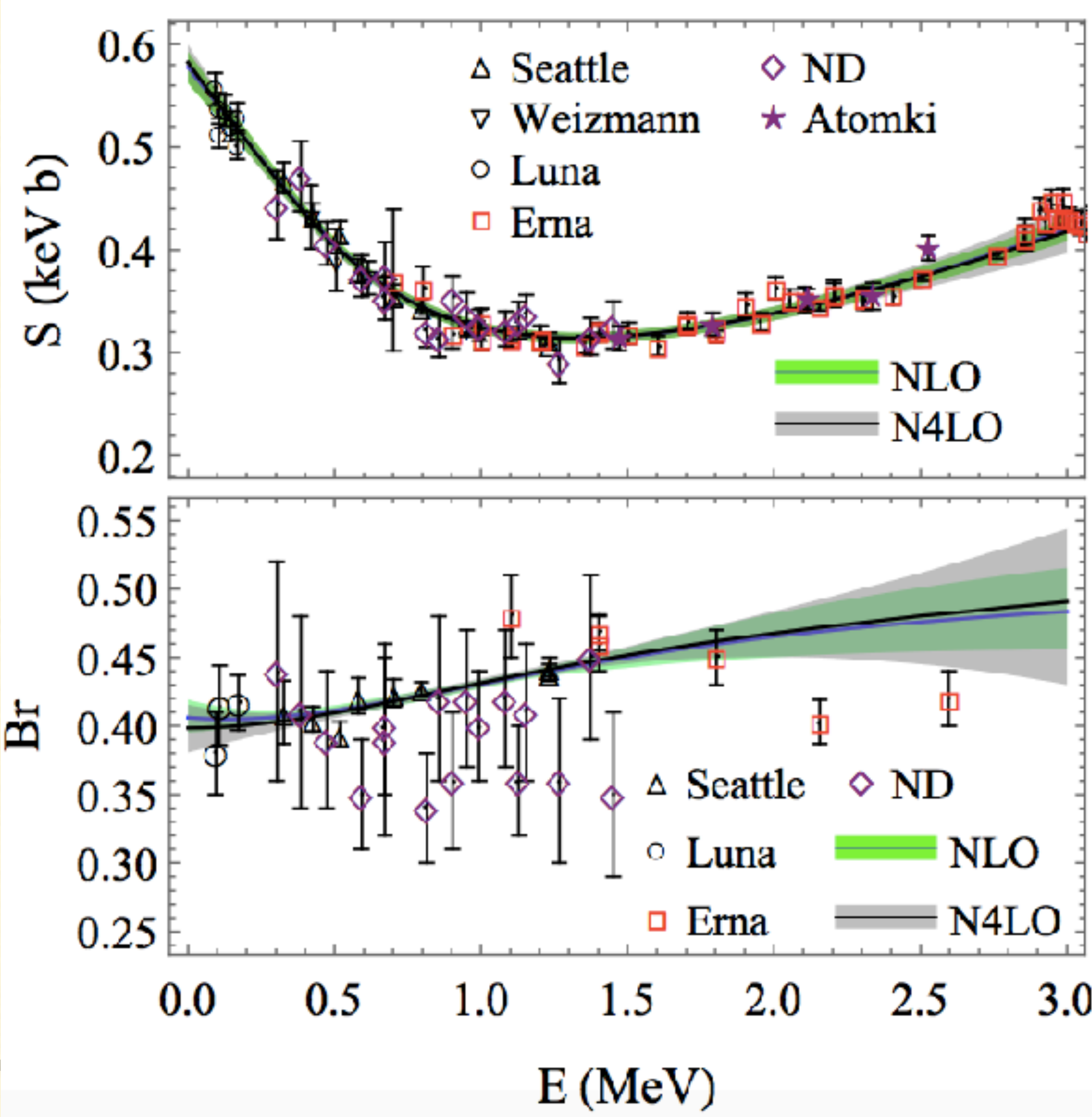

^{3}He(^{4}He,ɣ) results

Zhang, Nollett, DP, JPG (2019)
cf. Higa, Rupak, Vaghani, EPJA (2018)

- E1 external direct capture to a shallow p-wave bound state
- Only one spin channel
- Integral is not dominated by as large r as in ^{7}Be(p,ɣ)
- More sensitivity to ^{3}He-^{4}He scattering parameterization
- Distribution peaks at $\chi^2 = 82$

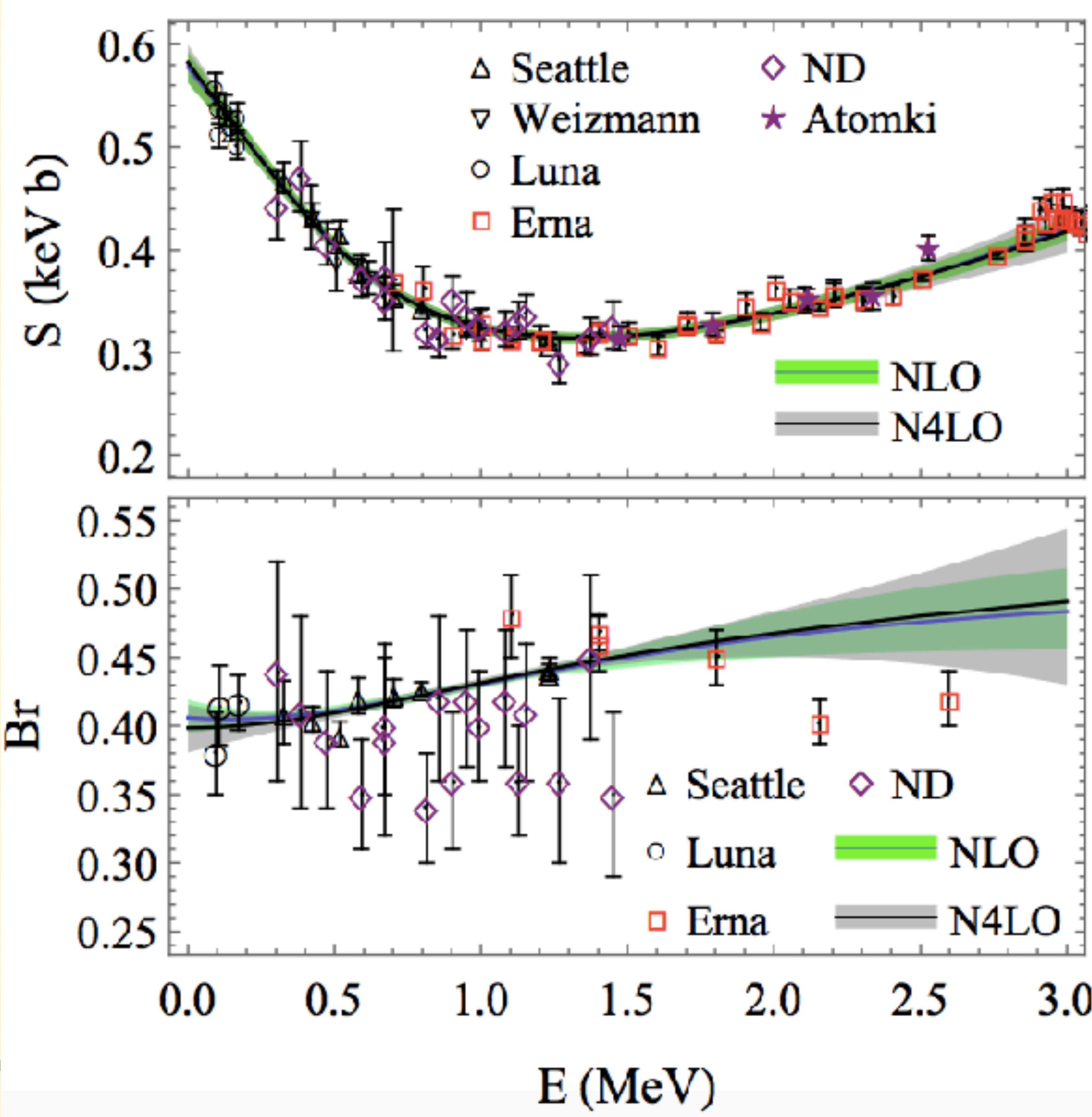

^{3}He(^{4}He,ɣ) results

Zhang, Nollett, DP, JPG (2019)
cf. Higa, Rupak, Vaghani, EPJA (2018)

- E1 external direct capture to a shallow p-wave bound state
- Only one spin channel
- Integral is not dominated by as large r as in ^{7}Be(p,ɣ)
- More sensitivity to ^{3}He-^{4}He scattering parameterization
- Distribution peaks at $\chi^2 = 82$
- Bayesian evidence ratio≅6 for NLO cf. N^{4}LO

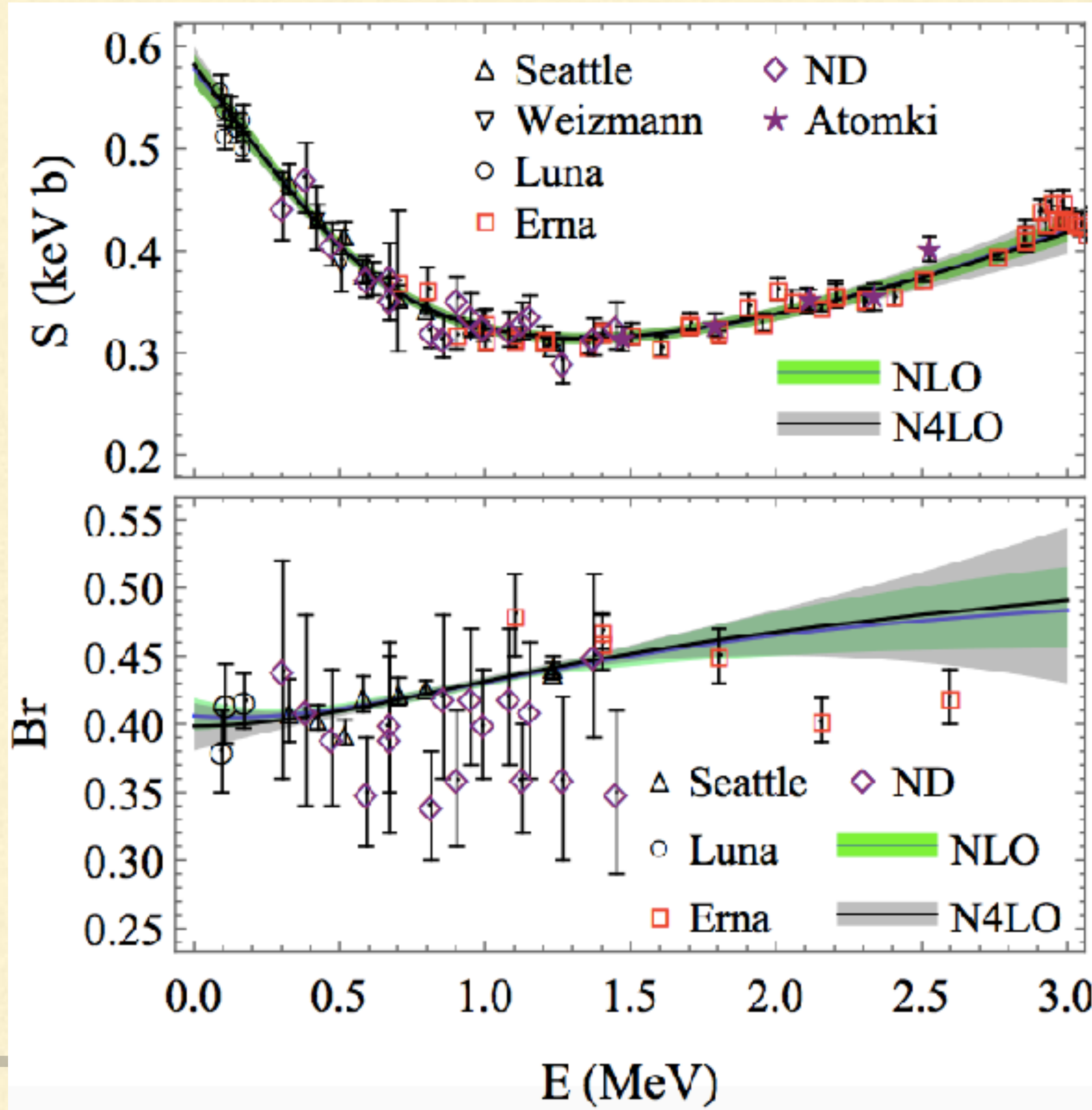

EFT treatment of ^{3}He + ^{4}He scattering

Poudel, Phillips, JPG (2022)

- Analyze SONIK data, Barnard data, and Boykin et al. A_y data
- Using Halo EFT to N2LO, $O(Q^2)$

$$Q = \frac{(p,q)}{\Lambda}$$

- $1/2^+$: a_0, r_0
- $1/2^-$, $3/2^-$: a_1, r_1, P_1 ($\Leftrightarrow E_{7Be}$, ANC, P_1)

Λ=200 MeV

- $7/2^-$: Resonance at E_{cm}=2.98 MeV with fitted Γ (R-matrix form)
- Likelihood: includes theory uncertainty based on convergence pattern of EFT expansion.

$$\Sigma^{\rm th}_{\alpha\beta} = (\Delta y)_\alpha (\Delta y)_\beta$$

$$\mathscr{L} \propto \exp\left(-\frac{1}{2}\vec{r}^T(\Sigma^{\rm th} + \Sigma^{\rm exp})\vec{r}\right)$$

$$r_{j\alpha} = y_{j\alpha} - f_\alpha \mu(x_{j\alpha}; \theta_{\rm EFT})$$

$$\Delta y_\alpha = y_{\rm ref}\bar{c}Q_\alpha^{\nu+1}$$

Pick data sets

- Scattering data
  - SONIK*: 451 from 0.385 to 2.7 MeV
  - Barnard: 646 from 1.49 to 2.7 MeV
  - Boykin et al.: 9 A_y data from 2.1 to 2.7 MeV

- Specify CMEs
  - SONIK: by energy
  - Barnard: 5%

*Paneru et al., submitted to Phys. Rev. C; Paneru, Ohio University Ph.D. thesis, 2020

SONIK data, with truncation uncertainty

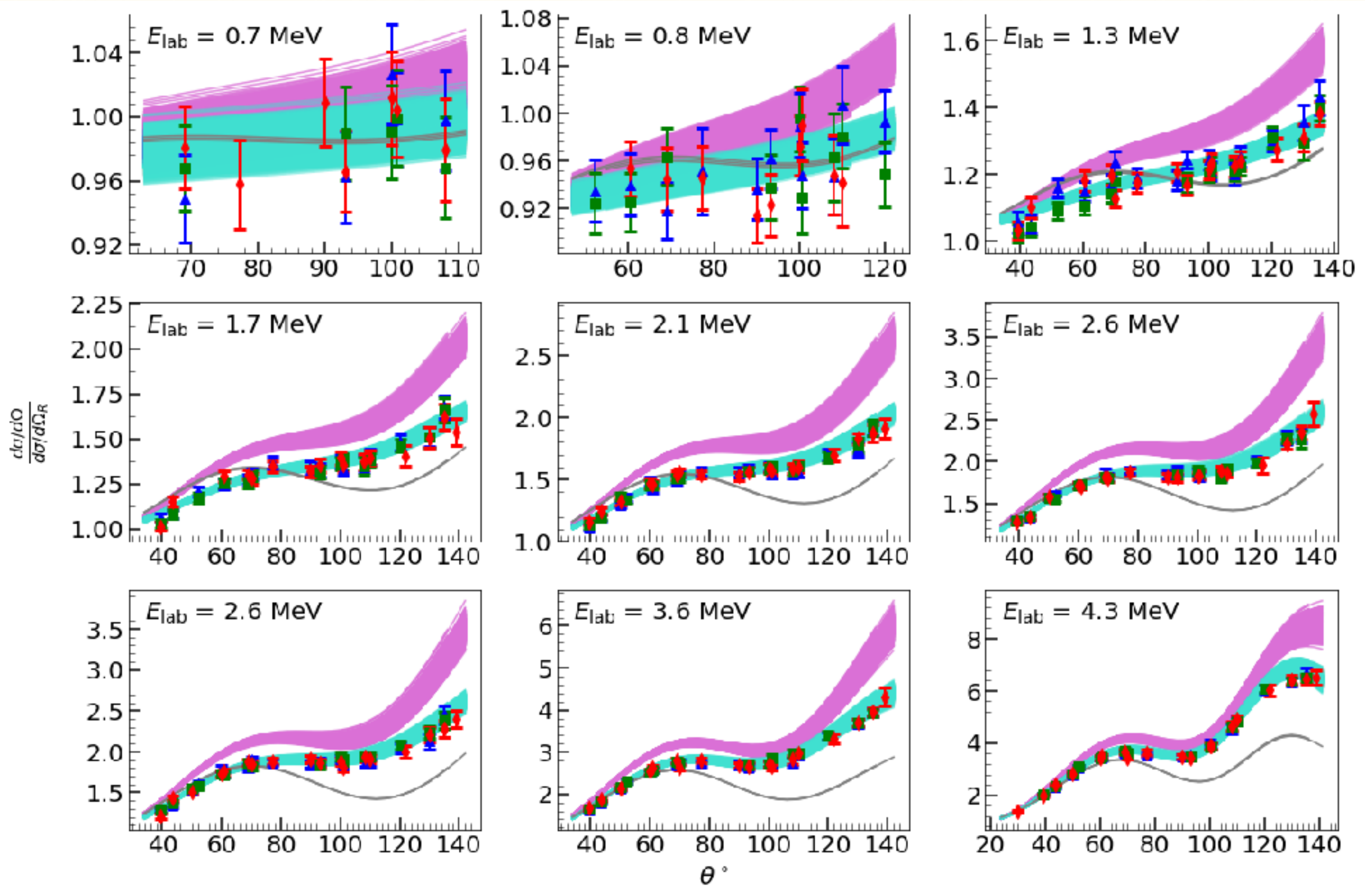

ERT parameters from scattering data

- Imposed prior on ANCs from capture data, so not *solely* from scattering data
- Consistent values: $C_1^{+2} = 15.5 \pm 1.5$ fm; $C_1^{-2} = 14.1 \pm 1.7$ fm
- $a_0 = 60^{+6}_{-5}$ fm cf. $a_0 = 50^{+7}_{-6}$ fm from capture and lower number from R-matrix

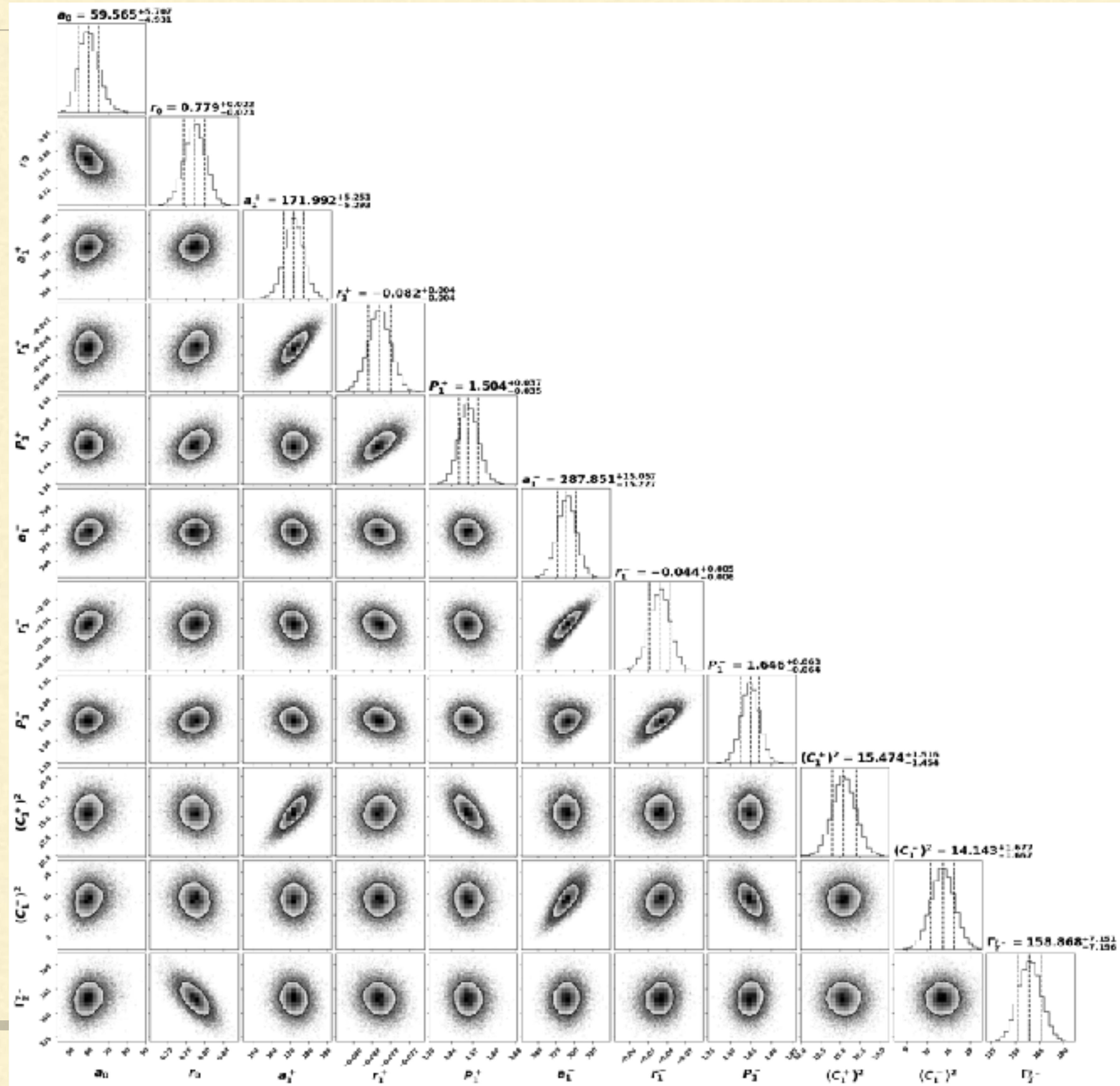

Inclusion of $7/2^-$ and $5/2^-$ resonances in Halo EFT

Burnelis, Phillips

- Analyze SONIK data
- Using Halo EFT to N2LO, $O(Q^3)$
- $1/2^+$: a_0, r_0, P_0
- $1/2^-$, $3/2^-$: a_1, r_1, P_1 ($\Leftrightarrow E_{7Be}$, ANC, P_1)
- $7/2^-$: Resonance at E_{cm}=2.98 MeV with form given by effective-range theory up to fourth order⇒width fitted to data
- $5/2^-$: fit effective-range theory up to second order to Boykin phase shifts and take as fixed
- Likelihood: includes theory uncertainty based on convergence pattern of EFT expansion.

Cross sections

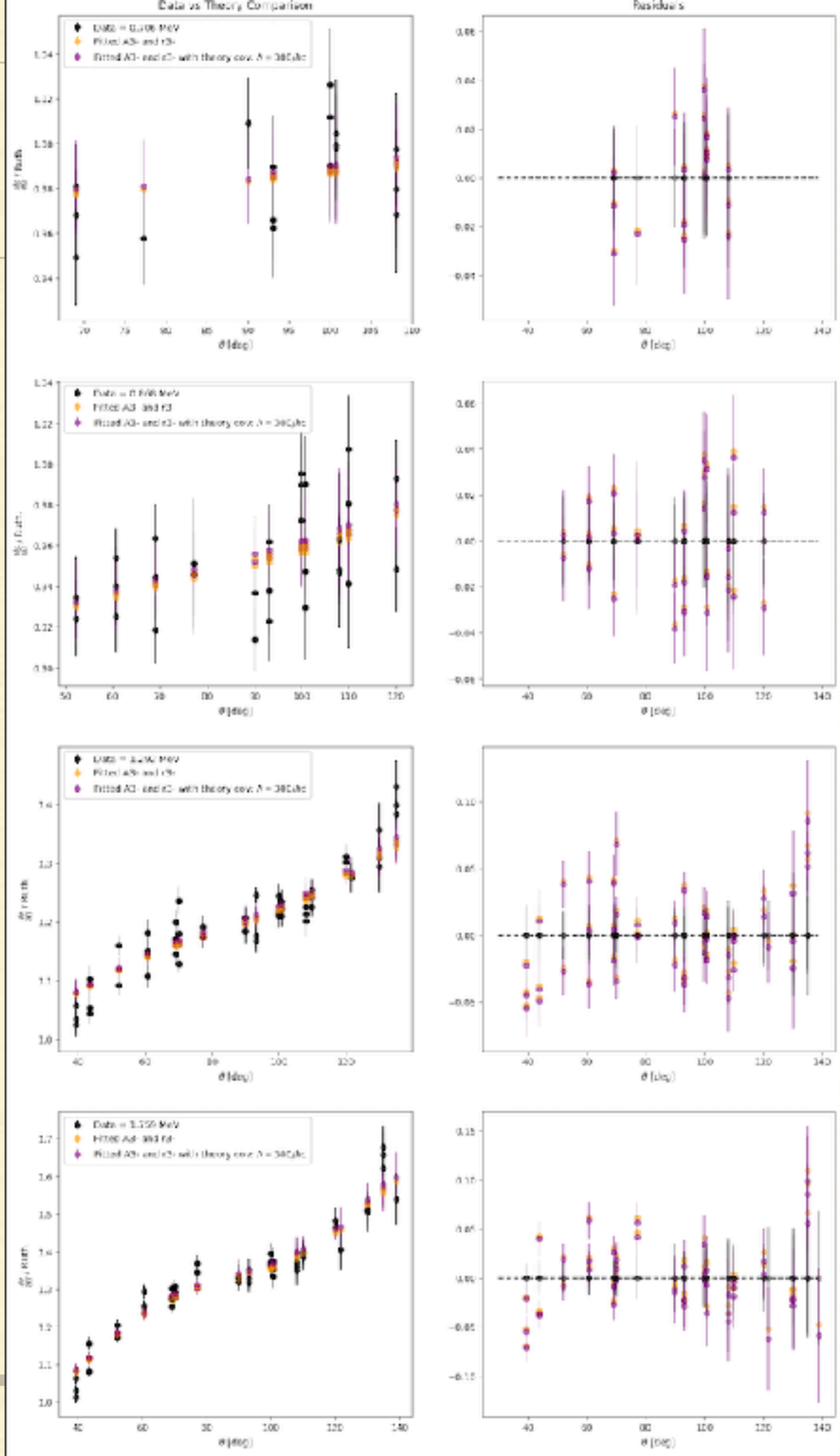

Cross sections

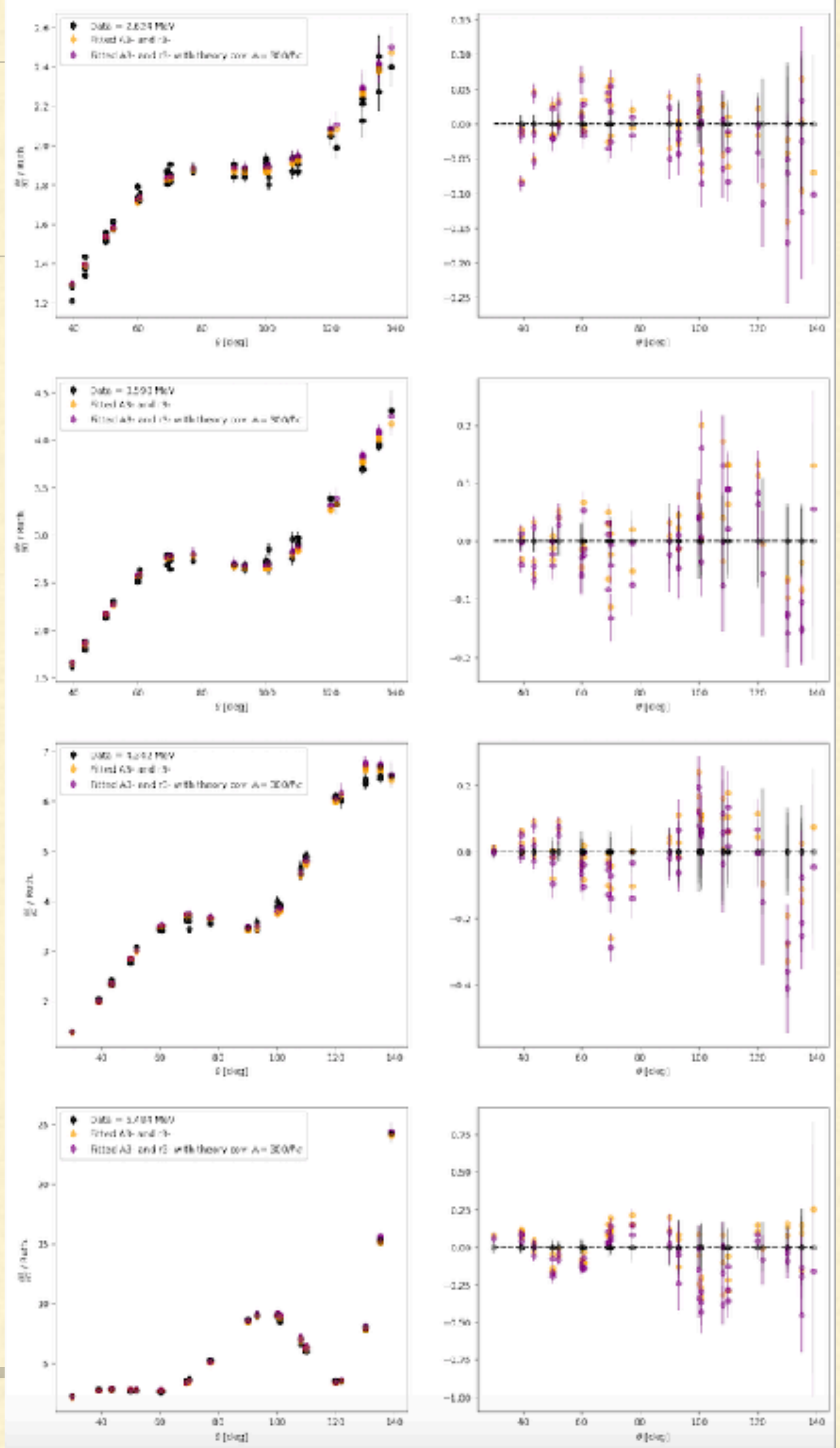

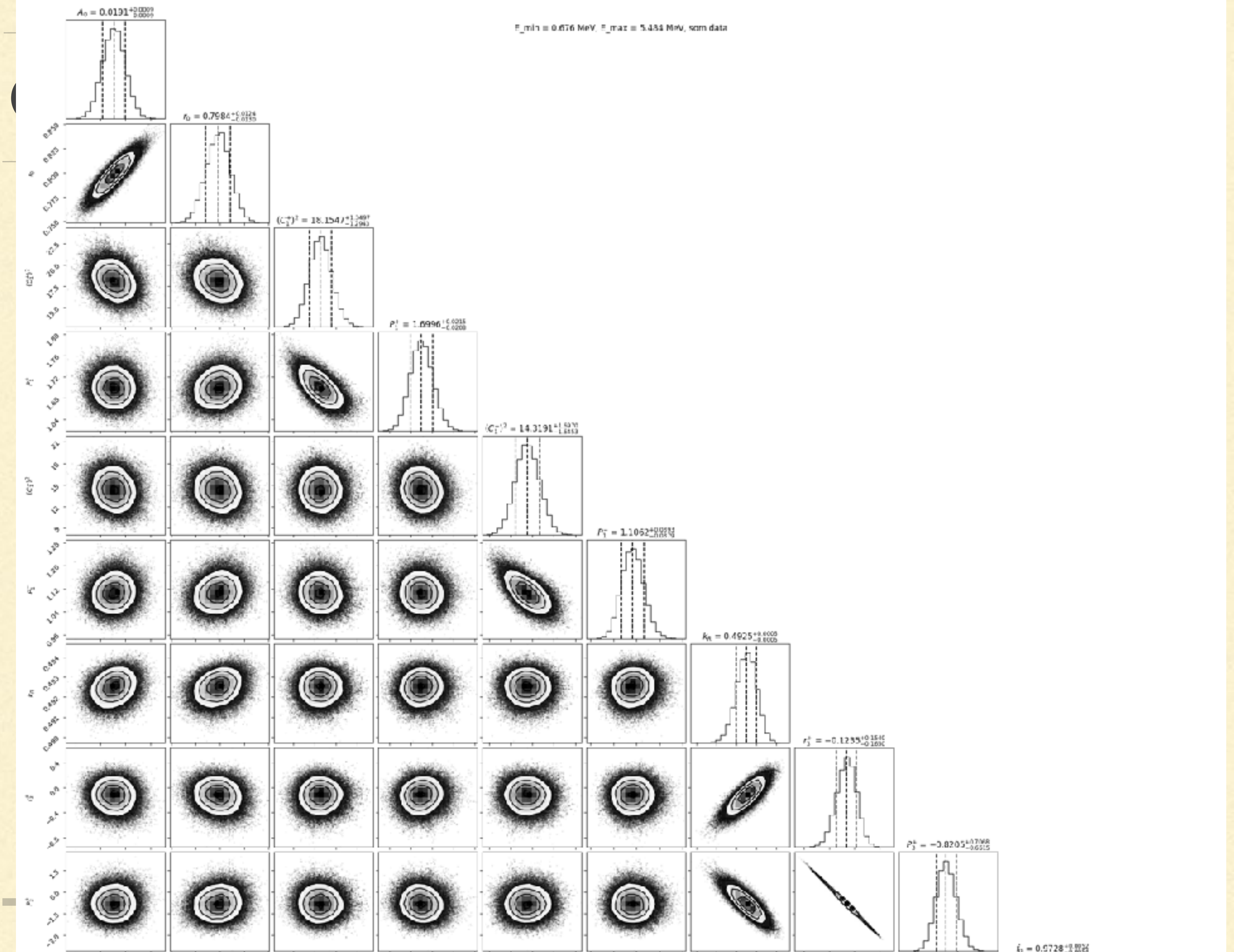
A_0 = 0.0191
r_0 = 0.7984
(C_1^+)^2 = 18.1547
P_1^+ = 1.6996
(C_1^-)^2 = 14.3191
P_1^- = 1.1062
k_R = 0.4925
r_1^S = −0.1255
P_1^S = −0.8205

Further applications of BRICK

- $^{19}F(p,\gamma)^{20}Ne$ – Zhang et al. (incl. deBoer, Odell) Nature **610**, 656-660 (2022)
    - Low-energy resonance opens up possibility of "warm" CNO breakout
- $^{10}B(p,\alpha)^{7}Be$ – Van de Kolk et al. (incl. deBoer, Odell) PRC **105**, 055802 (2022)
    - possible temperature probe for $^{11}B(p,2\alpha)^{4}He$ – aneutronic plasma fusion source
- $^{23}Na(p,\gamma)^{24}Mg$ – Boeltzig et al. (incl. deBoer, Odell) PRC **106**, 045801 (2022)
    - breakout reaction linking NeNa and MgAl cycles
- $^{13}C(\alpha,n_1)^{16}O$ – deBoer et al. (incl. deBoer, Odell) PRC **106**, 055808 (2022)
    - partial cross section measurement, improves BG modeling

Summary

- Parametric uncertainties in R-matrix analyses can be quantified by MCMC sampling of the Bayesian posterior and evaluating derived quantities
- https://github.com/odell/brick

- Multiple examples of successful application to different reactions
- Enables more sophisticated modeling of experimental imperfections
- Knowledge of full posterior provides access to parameter correlations, allows diagnosis of which parameters are not needed, shows where there is multi-modality, non-Gaussianity, and more
- Error propagation to derived quantities is straightforward with samples in hand
- Model checking (residuals, coverage, etc.) needs to be done at end
- Model uncertainties of R-matrix analysis? Comparison to EFT, ab initio, etc.